Development 130, 4161-4175

doi:10.1242/dev.00621

Selective degradation of excess Ldb1 by Rnf12/RLIM confers proper Ldb1 expression levels and Xlim-1/Ldb1 stoichiometry in *Xenopus* organizer functions

Ichiro Hiratani[1,2], Naoko Yamamoto[1], Toshiaki Mochizuki[1,*], Shin-ya Ohmori[1,2] and Masanori Taira[1,2,†]

[1]Department of Biological Sciences, Graduate School of Science, University of Tokyo, and [2]Core Research for Evolutional Science and Technology (CREST), Japan Science and Technology Corporation (JST), 7-3-1 Hongo, Bunkyo-ku, Tokyo 113-0033, Japan
*Present address: Department of Molecular Pathology, Graduate School of Medicine, University of Tokyo, 7-3-1 Hongo, Bunkyo-ku, Tokyo 113-0033, Japan
†Author for correspondence (e-mail: m_taira@biol.s.u-tokyo.ac.jp).

Accepted 21 May 2003

SUMMARY

The *Xenopus* LIM homeodomain (LIM-HD) protein, Xlim-1, is expressed in the Spemann organizer and cooperates with its positive regulator, Ldb1, to activate organizer gene expression. While this activation is presumably mediated through Xlim-1/Ldb1 tetramer formation, the mechanisms regulating proper Xlim-1/Ldb1 stoichiometry remains largely unknown. We isolated the *Xenopus* ortholog (XRnf12) of the RING finger protein Rnf12/RLIM and explored its functional interactions with Xlim-1 and Ldb1. Although XRnf12 functions as a E3 ubiquitin ligase for Ldb1 and causes proteasome-dependent degradation of Ldb1, we found that co-expression of a high level of Xlim-1 suppresses Ldb1 degradation by XRnf12. This suppression requires both the LIM domains of Xlim-1 and the LIM interaction domain of Ldb1, suggesting that Ldb1, when bound to Xlim-1, escapes degradation by XRnf12. We further show that a high level of Ldb1 suppresses the organizer activity of Xlim-1/Ldb1, suggesting that excess Ldb1 molecules disturb Xlim-1/Ldb1 stoichiometry. Consistent with this, Ldb1 overexpression in the dorsal marginal zone suppresses expression of several organizer genes including postulated Xlim-1 targets, and importantly, this suppression is rescued by co-expression of XRnf12. These data suggest that XRnf12 confers proper Ldb1 protein levels and Xlim-1/Ldb1 stoichiometry for their functions in the organizer. Together with the similarity in the expression pattern of *Ldb1* and *XRnf12* throughout early embryogenesis, we propose Rnf12/RLIM as a specific regulator of Ldb1 to ensure its proper interactions with LIM-HD proteins and possibly other Ldb1-interacting proteins in the organizer as well as in other tissues.

Key words: *Xenopus*, Spemann organizer, Protein-protein interactions, stoichiometry, E3 ubiquitin ligase, Proteasome, RING finger protein, LIM homeodomain protein, *XRnf12*/*RLIM*, *Ldb1*, *Xlim-1*

INTRODUCTION

The Spemann organizer plays a central role in body axis determination in vertebrates. It possesses the ability to direct surrounding cells to specific characters, namely dorsalization of mesoderm, neuralization of ectoderm, and anteroposterior patterning of these tissues (Harland and Gerhart, 1997; De Robertis et al., 2000; Bouwmeester, 2001), which are thought to be mediated by secreted antagonists for peptide growth factors such as BMPs, Wnts and Nodals (Harland and Gerhart, 1997; De Robertis et al., 2000). Their gene expression is supposedly regulated by several transcriptional activators expressed in the organizer region (Harland and Gerhart, 1997; Bouwmeester, 2001). The LIM homeodomain (LIM-HD) protein Xlim-1 is one of the important transcriptional activators specifically expressed in the organizer (Taira et al., 1992; Taira et al., 1994a; Taira et al., 1994b; Agulnick et al., 1996; Breen et al., 1998; Hiratani et al., 2001). In mice, *Lim1* null embryos exhibit a striking headless phenotype that lacks fore- and midbrain structures anterior to rhombomere 3 (Shawlot and Behringer, 1995). In *Xenopus*, Xlim-1 is also required for head formation (Nakano et al., 2000; Kodjabachian et al., 2001). Among the targets of Xlim-1 are organizer genes such as *goosecoid* (*gsc*), *chordin* (*chd*), and *Xotx2*, the expression of which is upregulated by Xlim-1 in the presence of its positive regulator, Ldb1 (LIM-domain-binding protein 1) in animal caps (Taira et al., 1994b; Agulnick et al., 1996; Taira et al., 1997; Mochizuki et al., 2000). *chordin* encodes a secreted BMP inhibitor (Sasai et al., 1995), which is likely to mediate the neural inducing activity of Xlim-1 (Taira et al., 1994b; Agulnick et al., 1996).

LIM-HD proteins have two highly conserved LIM domains in their N termini, which are involved in protein-protein interactions (Dawid et al., 1998; Bach, 2000). The LIM domains have been shown to produce negative regulatory effect on Xlim-1 (Taira et al., 1994b). Binding of cofactors to

the LIM domains is thought to relieve the inhibitory effect of the LIM domains on Xlim-1; Ldb1 (also known as NLI and CLIM2) being one such factor (Agulnick et al., 1996; Jurata et al., 1996; Bach et al., 1997). Ldb1 contains a self-dimerization domain and a LIM interaction domain (Jurata and Gill, 1997; Breen et al., 1998), and a dimer of Ldb1 has been shown to bridge two LIM-HD molecules (Lhx3/Lim3, Isl1, or Isl3) to form a tetrameric complex (Jurata et al., 1998). In the *Drosophila* wing disc, overexpression of Chip, the *Drosophila* ortholog of Ldb1, results in wing malformation, which is rescued by co-expression of the LIM-HD protein Apterous, suggesting that the stoichiometric ratio between LIM-HD and Ldb proteins is critical for LIM-HD activity (Fernandez-Funez et al., 1998; Milan and Cohen, 1999; van Meyel et al., 1999; Rincon-Limas et al., 2000). Tetrameric complex formation has also been supported by the observations that chimeric molecules in which the dimerization domain of Chip or Ldb1 is fused to a LIM domain-deleted construct of Apterous or Xlim-1, respectively, are as functional as co-expressed wild-type molecules (Milan and Cohen, 1999; van Meyel et al., 1999; Rincon-Limas et al., 2000; Hiratani et al., 2001). Thus, LIM-HD proteins are likely to function as a tetrameric complex with Ldb1 in a number of developmental contexts, but the mechanisms regulating the stoichiometric ratio between LIM-HD factor and Ldb1 are largely unknown.

In mice, a novel regulator for the LIM-HD transcription factor Lhx3, RLIM (also referred to as Rnf12 according to mouse gene nomenclature), has been isolated and shown to be capable of suppressing the activity of Lhx3 (Bach et al., 1999). Rnf12 contains a RING finger motif at its C terminus, which is a conserved, cysteine-rich, zinc-binding motif found in a diverse group of ubiquitin (Ub) ligases that mediate the transfer of Ub to heterologous substrates (Jackson et al., 2000; Joazeiro and Weissman, 2000). Ub ligases (E3) are determinants of target specificity in the protein ubiquitination pathway. After Ub is transferred from a Ub-activating enzyme (E1) to a Ub-conjugating enzyme (E2), Ub ligases (E3) promotes transfer of Ub from Ub-conjugating enzyme (E2) to a specific target protein, which is subsequently degraded by the proteasome (Hershko and Ciechanover, 1998; Glickman and Ciechanover, 2002). Suppression of LIM-HD factors by Rnf12 possibly relies on this activity, which has proved to be the case from recent work by Ostendorff et al. (Ostendorff et al., 2002), in addition to its proposed role in recruiting the histone deacetylase complex (Bach et al., 1999). Thus, Rnf12/RLIM appears to be a negative regulator for LIM-HD/Ldb1 complexes.

To determine whether Rnf12 also plays any role in the regulation of Xlim-1, we isolated the *Xenopus* ortholog *XRnf12* and examined its functional interactions with Xlim-1 and Ldb1 in early *Xenopus* development. Developmental expression analysis of *XRnf12* in comparison with *Xlim-1* and *Ldb1* revealed that the three genes are co-expressed in the Spemann organizer, raising the possibility that XRnf12 does not simply function as a negative regulator for Xlim-1. Our biochemical and functional analyses show that XRnf12 initiates ubiquitin-proteasome-dependent degradation of excess Ldb1 but not Ldb1 bound to Xlim-1 nor Xlim-1 itself, suggesting a role for XRnf12 in adjustment of Xlim-1/Ldb1 stoichiometry in the organizer by assuring proper Ldb1 expression levels.

MATERIALS AND METHODS

Embryo manipulations, preparation of synthetic mRNAs and RNA injections

Xenopus embryo manipulations were carried out as described (Hiratani et al., 2001). Template preparations, and synthesis and quantification of mRNAs have been described (Hiratani et al., 2001). Embryos were injected with RNA (10 nl/embryo) and incubated until the sibling embryos reached the appropriate stages. Animal caps were dissected at stage 8-9, cultured, and collected at the gastrula stage for further analysis.

Cloning of *XRnf12*

PCR with degenerate primers, dF4 and dR5, was carried out using a *Xenopus* neurula (stage 17/18) cDNA library (J. Shinga and M.T., unpublished). Primers were designed based on the conserved amino acid sequences in mouse and chick Rnf12: forward primer dF4, 5′-CA(A/G)AT(A/C/T)ATGACIGG(A/C/G/T)TT-(C/T)GG-3′ (I, inosine), which corresponds to the amino acid sequence QIMTGFG of XRnf12, and reverse primer dR5, 5′-TT(A/G)TC(A/G/T)AT-(C/T)TG(C/T)TC(C/T)TT-3′, which corresponds to the sequence KEQIDN of XRnf12. An amplified 0.36 kb fragment was cloned and used as a probe to screen a *Xenopus* gastrula cDNA library (a kind gift from B. Blumberg).

Plasmid constructs

The following plasmids were constructed and used for mRNA injections. To make pCS2+XRnf12, a PCR-amplified, *Nco*I-digested XRnf12 coding region was subcloned into *Nco*I-*Stu*I-digested pCS2+AdN (Mochizuki et al., 2000). pCS2+XRnf12(HC>AA) was generated by replacing His585 and Cys588 of XRnf12 with alanines using the Gene Editor in vitro Site-Directed Mutagenesis System (Promega). pCS2+Xlim-1-FLAG contains the Xlim-1 coding region flanked by a single FLAG epitope tag at the C terminus. pCS2+FLAG-Ldb1 contains the Ldb1 coding region downstream of a single FLAG epitope tag derived from pCS2+FTn (formerly pCS2+FLAG) (Mochizuki et al., 2000). pCS2+FLAG-Ldb1ΔC was constructed by replacing Ldb1 with Ldb1ΔC [formerly Ldb1(1-291)] (Hiratani et al., 2001). For pCS2+3HA-ubiquitin, a single copy of the *Xenopus* ubiquitin was PCR-amplified from a *Xenopus* neurula cDNA library and subcloned into *Eco*RI-*Xba*I-digested pCS2+3HA, which provides three N-terminal HA epitope tags. Primer sequences were based on the second ubiquitin repeat sequence of pXlgC20 (Dworkin-Rastl et al., 1984) and are as follows: forward, 5′-ggaattctATGCAGATCTTT-GTAAAA-3′ (lower case, linker sequences; underline, restriction site); reverse, 5′-gctctagaCTAGCCACCCCTGAGCCGAAG-3′. pCS2+NLS-ABL60, pCS2+NLS-CT239, and pCS2+NLS-CT261 contain amino acids 1-177, 239-403, and 261-403 of Xlim-1, respectively, downstream of the SV40 large T antigen NLS (MAPKKKRKV). pCS2+HD34 contains amino acids 178-272 of Xlim-1. pCS2+LMO2 contains full-length mouse LMO2 amplified by PCR. pCS2+hRNF6, pCS2+hRNF13, and pCS2+hRNF38 were constructed with pCS2+ by PCR amplification of the entire coding region from cDNA clones (GenBank accession numbers: BC034688, BC009781, and BC033786, respectively) provided by the Mammalian Gene Collection (MGC) project (NIH) through Open Biosystems. pSP64-Xβm (*Xenopus* β-globin) has been described (Krieg and Melton, 1984).

The following plasmids were used for GST pull-down assays. pGEX2TNEX-XRnf12ΔC and pGEX2TNEX-XRnf12ΔN contain amino acids 1-283 and 282-616, respectively, of XRnf12 in pGEX2TNEX (Hiratani et al., 2001). pGEX2T-Ldb1 contains full-length Ldb1 in pGEX2T. pGEX2T-ABL60, pGEX2T-ΔC, pGEX2T-CT239, pGEX2T-ΔNA, and pGEX2T-Xlim-1 contain portions of Xlim-1 shown in Fig. 5E in pGEX2T. pGEX2T-HD27 has been described previously [formerly GST/Xlim-1(HD27)] (Mochizuki et al., 2000). pSP64T-Xlim-5 was constructed as follows: the coding

region of Xlim-5 was obtained from pBluescript-KS(+)Xlim-5 plasmid (Toyama et al., 1995) by *Pvu*II-*Hin*cII digestion, and inserted into end-filled *Bgl*II site of pSP64T (Krieg and Melton, 1984). pSP64T-Xlim-3 has been described previously (Yamamoto et al., 2003). All constructs were verified by sequencing.

GST (glutathione S-transferase) pull-down assay

Generation of GST fusion proteins, in vitro translation, and GST pull-down assay were carried out as described previously (Mochizuki et al., 2000; Hiratani et al., 2001), except for the use of approximately 5 μg of GST fusion proteins per assay. For in vitro translation, pCS2+Xlim-1 (Hiratani et al., 2001), pSP64T-Xlim-3, pSP64T-Xlim-5, pSP64RI-XLdb1 (Agulnick et al., 1996), pCS2+Ldb1ΔC, pCS2+XRnf12, pCS2+hRNF6, pCS2+hRNF13 and pCS2+hRNF38 were used.

Northern blot and RT-PCR analysis

Northern blot analysis was performed using the stored original blot from the previous study (Hikasa and Taira, 2001). A 0.36 kb PCR fragment amplified with degenerate primers dF4 and dR5, which contained the *XRnf12C* sequence, was cloned into the pT7Blue vector (Novagen), excised with *Nde*I-*Eco*RI, gel-purified, and used as a *XRnf12* probe. RT-PCR analysis was done as described previously (Osada et al., 2003).

Nuclear β-gal staining, whole-mount in situ hybridization and sectioning

For lineage tracing, nβ-gal mRNA transcribed from linearized pCS2+nβ-gal was co-injected and visualized by Red-Gal (Research Organics) staining. Whole-mount in situ hybridization was carried out as described previously (Harland, 1991; Shinga et al., 2001). For hemisections, rehydrated embryos were embedded in 2% low melt agarose in 1× PBS containing 0.3 M sucrose and 0.05% Triton X-100, and sectioned with a razor blade before hybridization as described previously (Lee et al., 2001). Digoxigenin-labeled antisense RNA probes were transcribed from *Xlim-1* (Taira et al., 1992), *gsc* (Cho et al., 1991), *chd* (Sasai et al., 1995), *Xotx2* (Pannese et al., 1995), *XPAPC* (Kim et al., 1998), *cer* (Bouwmeester et al., 1996), *XFKH1* (Dirksen and Jamrich, 1992), *Xnot* (von Dassow et al., 1993), *Mix.1* (Rosa, 1989) and *Xbra* (Smith et al., 1991) plasmid templates. PCR-amplified template containing a T7 promoter sequence was used for *dkk1* (Shibata et al., 2001). pBluescript-SK(–)XRnf12 and pBluescript-SK(–)XLdb1 (Agulnick et al., 1996) were used for *XRnf12* and *Ldb1* probes, respectively.

Albino embryos were stained slightly more intensively than usual for better interior staining and embedded in paraffin wax and sectioned. Nuclei were stained with DAPI (4′,6-diamidino-2-phenylindole) as described previously (Shibata et al., 2001).

Protein extraction

Embryos were collected at the gastrula stage (stage 10.5 or 11) and homogenized in 10 μl of homogenizing buffer (50 mM Tris-HCl, pH 8.0, 50 mM KCl, 20% glycerol, 1 mM EDTA, 1 mM EGTA, 5 mM DTT, 1 mM PMSF) per embryo (or 2-2.5 μl per animal cap), and the supernatant was collected after centrifugation. For the dispersed cell experiments, mRNA-injected embryos were cultured in Ca^{2+}/Mg^{2+}-free 1× MBS containing 0.2% BSA and 50 μg/ml gentamicin sulfate in agarose-coated dishes, and vitelline membranes were removed at stage 6. Then, 50 μM (final) MG-132 (Peptide Institute), or an equal volume of DMSO for the negative control, was added to the medium and embryos were dispersed into single cells by gentle agitation. Cells were collected at the gastrula stage for preparation of cell lysates. Protein concentrations of the lysates were determined by a Protein Assay kit (Bio-Rad).

Western blot analysis and whole-mount immunostaining

For western blotting, equivalent amounts of total proteins were separated by SDS-PAGE, transferred to a PVDF membrane, and visualized either by chemical luminescence using the ECL system (Amersham Pharmacia) or by alkaline phosphatase staining using NBT/BCIP. Whole-mount immunostaining was done essentially as described previously (Hiratani et al., 2001), except for the use of ImmunoPure Metal-Enhanced DAB Substrate Kit (Pierce) for staining. Bisection of gastrula embryos were done as described previously (Lee et al., 2001). Antibodies used are as follows: anti-FLAG (M2, Sigma), anti-HA (12CA5, Roche), anti-β-tubulin (clone tub 2.1, Sigma), anti-Ldb1/CLIM2 (N-18, Santa Cruz), anti-Ldb1/NLI (Jurata et al., 1996), horseradish peroxidase (HRP)-conjugated anti-mouse Ig antibody from sheep (Amersham Pharmacia), alkaline phosphatase-conjugated anti-mouse IgG antibody from goat (Promega), HRP-conjugated anti-goat IgG from donkey (Santa Cruz), and HRP-conjugated anti-rabbit Ig from donkey (Amersham Pharmacia).

Coimmunoprecipitation assay

Coimmunoprecipitation assays were done essentially as described previously (Watanabe and Whitman, 1999), with slight modifications. Cell lysates were collected as described above except for the use of lysis buffer [20 mM Tris-HCl (pH 8.0), 1 mM EDTA, 10% glycerol, 8 mM DTT, 40 μg/ml leupeptin, 20 μg/ml aprotinin, 1 mM PMSF] containing 0.1% NP-40. Equivalent amounts of lysates (100-200 μl) were incubated with 1 μg of anti-FLAG antibody for 1 hour at 4°C, then added with 40 μl of protein G-agarose (Roche), and incubated for another 30 minutes at 4°C. After being washed 5 times with lysis buffer sequentially containing each of the following: (1) 0.1% NP-40, (2) 0.4 M NaCl, (3) 0.5% NP-40, (4) 0.2 M NaCl and 0.25% NP-40, and (5) nothing, SDS sample buffer was added and the bound proteins were eluted from beads by boiling. The eluted proteins were separated by SDS-PAGE, followed by western analysis.

RESULTS

Isolation and characterization of XRnf12

To determine whether Rnf12 plays any role in regulating the activity of Xlim-1, we isolated the *Xenopus Rnf12* ortholog by degenerate PCR procedure and subsequent screening of a *Xenopus* gastrula cDNA library. We obtained a clone encoding a protein of 616 amino acids that shared 65% and 70% identity with mouse and chick Rnf12, respectively. Based on phylogenetic comparison with the mouse, chick, and human Rnf12, and Rnf12-related proteins such as RNF6 (data not shown), we assume that this clone encodes the *Xenopus* ortholog of Rnf12, which we refer to as XRnf12 (Fig. 1A).

We also isolated two other genes highly related to *XRnf12*, named *XRnf12B* and *XRnf12C* (Fig. 1A,B). XRnf12B and XRnf12C share 89% identity with each other, and contain similar repetitive sequences of heptamer peptide of distinct sizes, the consensus of which is P-E/V-S-V-P/A-E/V. XRnf12B and XRnf12C may either be paralogs or alleles of XRnf12 because they both share 93% identity with XRnf12 outside of the repetitive sequence. Because XRnf12B and XRnf12C showed mRNA expression patterns and activities indistinguishable from XRnf12 in our studies (data not shown), we employed functional analyses that primarily used XRnf12, which is structurally closest to mouse Rnf12.

Because the N-terminal region of Rnf12 binds to both LIM-HD proteins and Ldb1/CLIM2 (Bach et al., 1999), we performed GST pull-down experiments with XRnf12, *Xenopus* LIM-HD proteins, and Ldb1. As expected, the N-terminal region [amino acids (aa) 1-283] of XRnf12 interacted

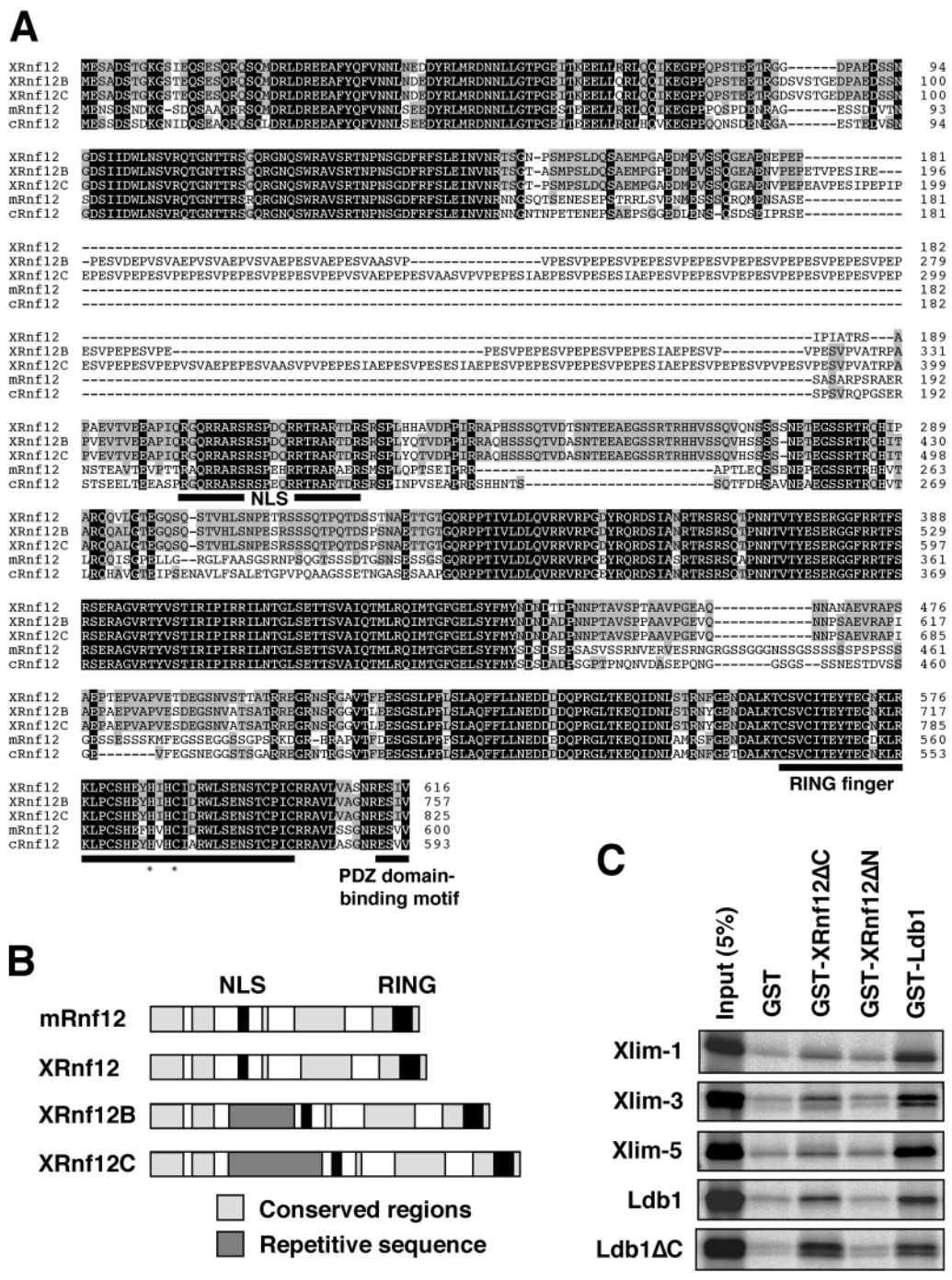

Fig. 1. Characterization of XRnf12. (A) Amino acid sequence alignment of XRnf12, XRnf12B, and XRnf12C, as well as mouse and chick Rnf12. Note the repetitive heptamers present in XRnf12B and XRnf12C. A PDZ domain-binding motif is present in the C terminus. NLS, nuclear localization signal; asterisks, sites of mutation in the RING mutant XRnf12(HC>AA). DDBJ Accession Numbers are: XRnf12 (AB114039), XRnf12B (AB114040) and XRnf12C (AB114041). (B) Schematic representation of mRnf12, XRnf12, XRnf12B, and XRnf12C. (C) The N-terminal region (aa 1-283) of XRnf12 interacts with LIM homeodomain proteins and Ldb1. GST pull-down assay was performed with ^{35}S-labeled Xlim-1, Xlim-3, Xlim-5, Ldb1 and Ldb1ΔC. While GST-XRnf12ΔC interacts with all of the proteins tested, GST-XRnf12ΔN shows little interaction. GST and GST-Ldb1 serves as negative and positive controls, respectively.

with Xlim-1, Xlim-3, Xlim-5, and Ldb1 (Fig. 1C, GST-XRnf12ΔC), while the C-terminal region (aa 282-616) of XRnf12 showed little or no interaction with any of them (Fig. 1C, GST-XRnf12ΔN). We also found that the N-terminal region (aa 1-291) of Ldb1 is sufficient for the interaction with XRnf12ΔC (Fig. 1C, Ldb1ΔC). Thus, XRnf12 possesses characteristics similar to mouse Rnf12 in terms of protein-binding specificity.

Expression of *XRnf12* overlaps with that of *Xlim-1* and *Ldb1* in the gastrula mesoderm

To evaluate temporal expression patterns of the *XRnf12* genes, we carried out northern analysis using a 359 base probe of *XRnf12C*, which shares 93% and 99% identity at the nucleotide level with *XRnf12* and *XRnf12B*, respectively, assuming that any of the three *XRnf12* genes could be detected with this probe. Two maternal *XRnf12* transcripts of different sizes (3.0 and 3.5 kb) were detected at the cleavage stage (Fig. 2A). While the 3.0 kb transcript disappeared at the gastrula stage (Fig. 2A, stage 11), the 3.5 kb transcript is maintained at relatively constant levels throughout early embryogenesis, with a slight increase at the late gastrula stage (Fig. 2A, stage 12.5). Judging from their size differences, the 3.0 kb and 3.5 kb transcripts may represent *XRnf12* and *XRnf12B/C* genes, respectively.

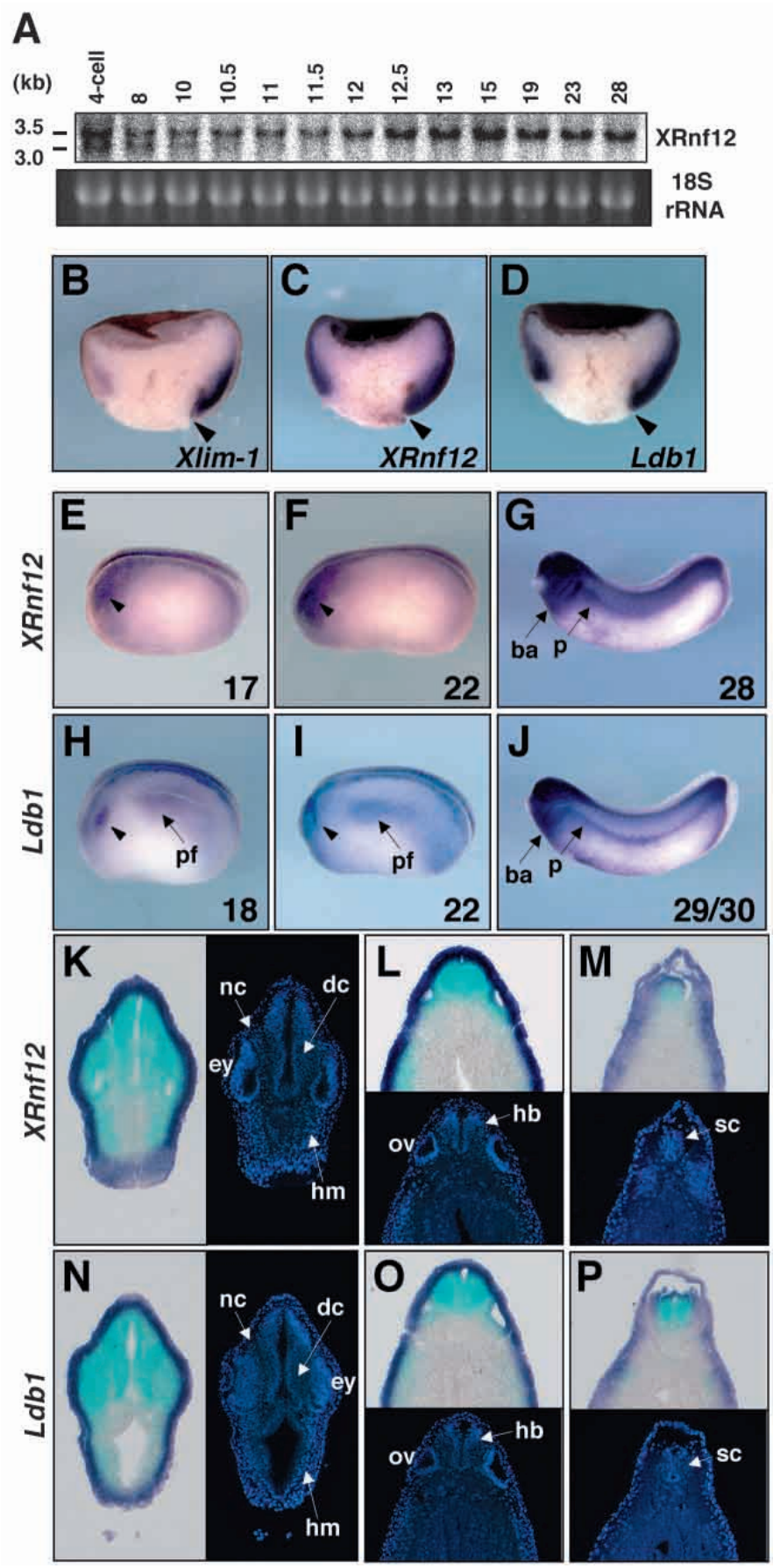

If XRnf12 plays any role in the regulation of Xlim-1 or Ldb1, it should be colocalized with Xlim-1 or Ldb1. Thus, we next carried out whole-mount in situ hybridization using sagittally bisected embryos to compare their mRNA expression patterns at the gastrula stage. *Xlim-1* mRNA was enriched in the dorsal mesoderm, with a faint expression also detected in the ventral mesoderm (Fig. 2B) as reported previously (Taira et al., 1992). *XRnf12* expression was detected in the entire mesoderm and ectoderm (Fig. 2C), and showed remarkable resemblance to *Ldb1* expression (Fig. 2D), consistent with the reported expression of *Rnf12* and *Ldb1* in mice (Bach et al., 1999) and *Ldb1* in *Xenopus* (Agulnick et al., 1996). Taken together, these results show that the three mRNAs colocalize in the gastrula mesoderm.

The similarity of *XRnf12* and *Ldb1* expression at the gastrula stage led us to further compare their expression during embryogenesis. After the gastrula stage, the expression of both transcripts is gradually restricted to tissues originated from the ectoderm, the neuroectoderm,

Fig. 2. Temporal and spatial expression patterns of *XRnf12*. (A) Northern analysis. The 3.5 kb transcript is expressed throughout early embryogenesis, while the 3.0 kb transcript disappears at stage 11. 18S rRNA stained with ethidium bromide served as a loading control. Numbers at the top are developmental stages. (B-D) Overlapping expression of *Xlim-1*, *XRnf12* and *Ldb1* in the gastrula mesoderm as revealed by whole-mount in situ hybridization of sagittally bisected gastrula embryos (stage 10.5). Animal side is to the top, dorsal to the right. Arrowhead, blastopore. (E-J) Co-expression of *XRnf12* and *Ldb1* in neurula and tailbud stage embryos. Dorsal is to the top, anterior to the left. Arrowhead indicates profundal-trigeminal placodal area; numbers in the bottom right of each panel are the developmental stages. (K-P) Co-expression of *XRnf12* and *Ldb1* as revealed by cross sections of stained tailbud embryos (stage 26). Upper, or left, panels are bright-field images; lower, or right, panels show DAPI staining. *XRnf12* (E-G,K-M) and *Ldb1* (H-J,N-P) are similarly expressed throughout early embryogenesis. Turquoise staining inside of the embryos shown in the cross sections resulted from BCIP staining as NBT was depleted by strong staining in the epidermis. Both genes are expressed similarly in the neural tube along the AP axis. ba, branchial arches; dc, diencephalon; ey, eye; hb, hindbrain; hm, head mesenchyme; nc, neural crest; ov, otic vesicle; p, pronephros; pf, pronephric field; sc, spinal cord.

neural crest and epidermis (data not shown), and subsequently to the neural tube as well as the head and the tailbud region (Fig. 2E-J). Additional expression of *Ldb1* is seen in the pronephric field, and the profundal-trigeminal placodal area (pPrV) (Schlosser and Northcutt, 2000) at the neural groove to neural tube stages (Fig. 2H,I, arrowhead). Although not as localized, *XRnf12* also appears to be present in the pPrV area (Fig. 2E,F, arrowhead). At the tailbud stage, expression of both genes is detected in the pronephric region and branchial arches (Fig. 2G,J). Cross sections of tailbud embryos confirmed their colocalization in the epidermis, neural crest, neural tube and head mesenchyme (Fig. 2K-P). These results show that the expression domains of *XRnf12* and *Ldb1* largely overlap throughout early embryogenesis, suggesting that the two genes may function in a common regulatory process rather than having distinct roles independent of each other (see Discussion).

XRnf12 suppresses secondary axis formation elicited by Xlim-1/Ldb1 and antagonizes organizer activity upon overexpression

Because *Xlim-1*, *Ldb1* and *XRnf12* transcripts colocalize in the gastrula mesoderm, we next asked whether XRnf12 could affect the axis-inducing activity of Xlim-1/Ldb1 (Agulnick et al., 1996). As shown in Fig. 3A, co-expression of XRnf12 markedly suppressed secondary axis formation elicited by Xlim-1/Ldb1, while β-globin, as negative control, had no effect. Notably, point mutations in the RING finger, which is supposed to abolish its zinc binding activity (Saurin et al., 1996), almost totally abolished the inhibitory action of XRnf12 (Fig. 3A, XRnf12(HC>AA)). We further examined the effect of overexpression of XRnf12 in the dorsal marginal zone. While XRnf12(HC>AA) had only a small effect (9% headless or cyclopic, *n*=118; Fig. 3B), overexpression of XRnf12 resulted in reduced head structures (52% headless or cyclopic, *n*=171; Fig. 3C), suggesting that XRnf12 is likely to interfere with organizer function through RING finger-dependent activity. This was also confirmed by downregulation of organizer gene expression by XRnf12 as described below.

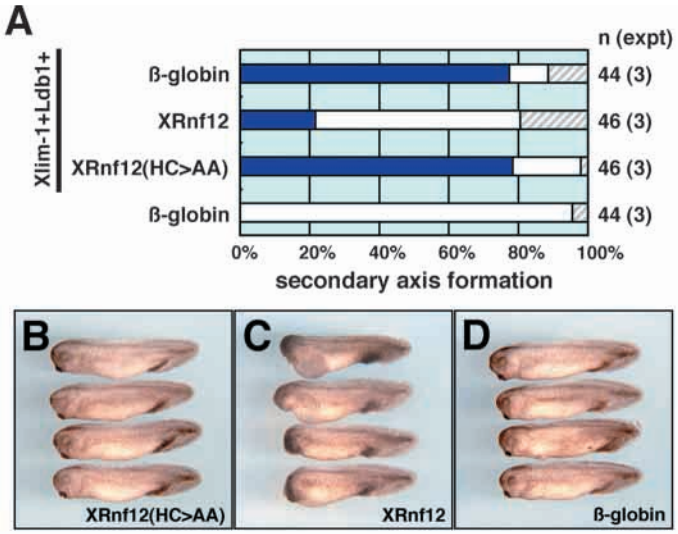

Fig. 3. XRnf12 suppresses axis duplication elicited by Xlim-1/Ldb1 and antagonizes head organizer activity in a RING-dependent manner. (A) XRnf12 blocks secondary axis formation elicited by Xlim-1/Ldb1, whereas the RING mutant XRnf12(HC>AA) does not. Embryos injected with the mRNAs indicated were scored for axis development at the tailbud stage and categorized as secondary axis (dark blue bars), normal (white bars), or others (hatched bars). β-globin serves as a negative control. n, total number of injected embryos; expt, number of independent experiments. Amounts of mRNAs injected (ng/embryo): Xlim-1, 0.25; Ldb1, 0.5; XRnf12 constructs, 0.25; β-globin (coinjected), 0.25; β-globin (alone), 1.0. (B-D) Overexpression of XRnf12 in the dorsal marginal zone leads to head defects. While XRnf12(HC>AA) has little or no effect (B), XRnf12 overexpression in the dorsal region results in reduced head structures (C). β-globin has no effect (D). Amounts of mRNAs injected were 2.0 or 4.0 ng/embryo.

XRnf12 mediates ubiquitination and proteasome-dependent degradation of Ldb1 but not Xlim-1

To examine whether specific protein degradation could account for the RING-dependent suppression by XRnf12, we examined the steady-state levels of FLAG-tagged Ldb1 or Xlim-1 overexpressed ventrally in the presence or absence of XRnf12. XRnf12 did not alter the steady-state level of Xlim-1-FLAG, either in the presence or absence of Ldb1 (Fig. 4A). Rather, we found that Ldb1 enhanced expression levels of Xlim-1-FLAG (Fig. 4A, compare lanes 4,5 with lanes 2,3; see Discussion). In contrast, XRnf12 caused marked reduction in the steady-state level of FLAG-Ldb1 (Fig. 4B, lanes 3,5) in a RING-dependent manner (Fig. 4B, lane 6), in good correlation with the RING-dependent suppression of axis duplication (Fig. 3A). We also noticed that the expression level of FLAG-Ldb1 was increased by Xlim-1 co-expression (Fig. 4B, compare lanes 2 and 4; further described below).

We next tested whether XRnf12 ubiquitinates Ldb1. FLAG-Ldb1 and HA-ubiquitin were co-expressed in the presence of XRnf12 and the lysates were immunoprecipitated with anti-FLAG antibody, followed by immunoblotting with anti-FLAG and anti-HA antibodies. Anti-FLAG immunoblotting confirmed that co-expression of XRnf12 results in downregulation of non-ubiquitinated FLAG-Ldb1 expression levels as expected (Fig. 4C, lower panel, lanes 6,7). While low amounts of ubiquitinated proteins, probably resulting from intrinsic ubiquitin ligase activity, were detected by anti-HA immunoblotting in the absence of XRnf12 (Fig. 4C, upper panel, lane 4), strong ladder-like signals, which probably correspond to polyubiquitin-conjugated Ldb1 products, appeared in the presence of XRnf12 (upper panel, lane 7), in contrast to the low amounts of non-ubiquitinated FLAG-Ldb1 present (lower panel, lane 7). As expected, XRnf12(HC>AA) did not enhance ubiquitination (Fig. 4C, compare lane 8 with lane 4), suggesting that the enhancement was RING dependent. By using FLAG-Ldb1ΔC, we obtained basically the same result except for the smaller sizes of the ubiquitinated protein bands (Fig. 4D), confirming that the ubiquitinated proteins in Fig. 4C are indeed Ldb1 but not some other proteins associated with FLAG-Ldb1. The results also suggest that the N-terminal region (aa 1-291) of Ldb1 is sufficient for the ubiquitination and degradation mediated by XRnf12. However, we also noticed that the degradation efficiency of Ldb1ΔC is somewhat lower than full-length Ldb1, possibly due to the lack of some residues present in the C-terminal region important for its ubiquitination and degradation. In contrast to Ldb1, we did not

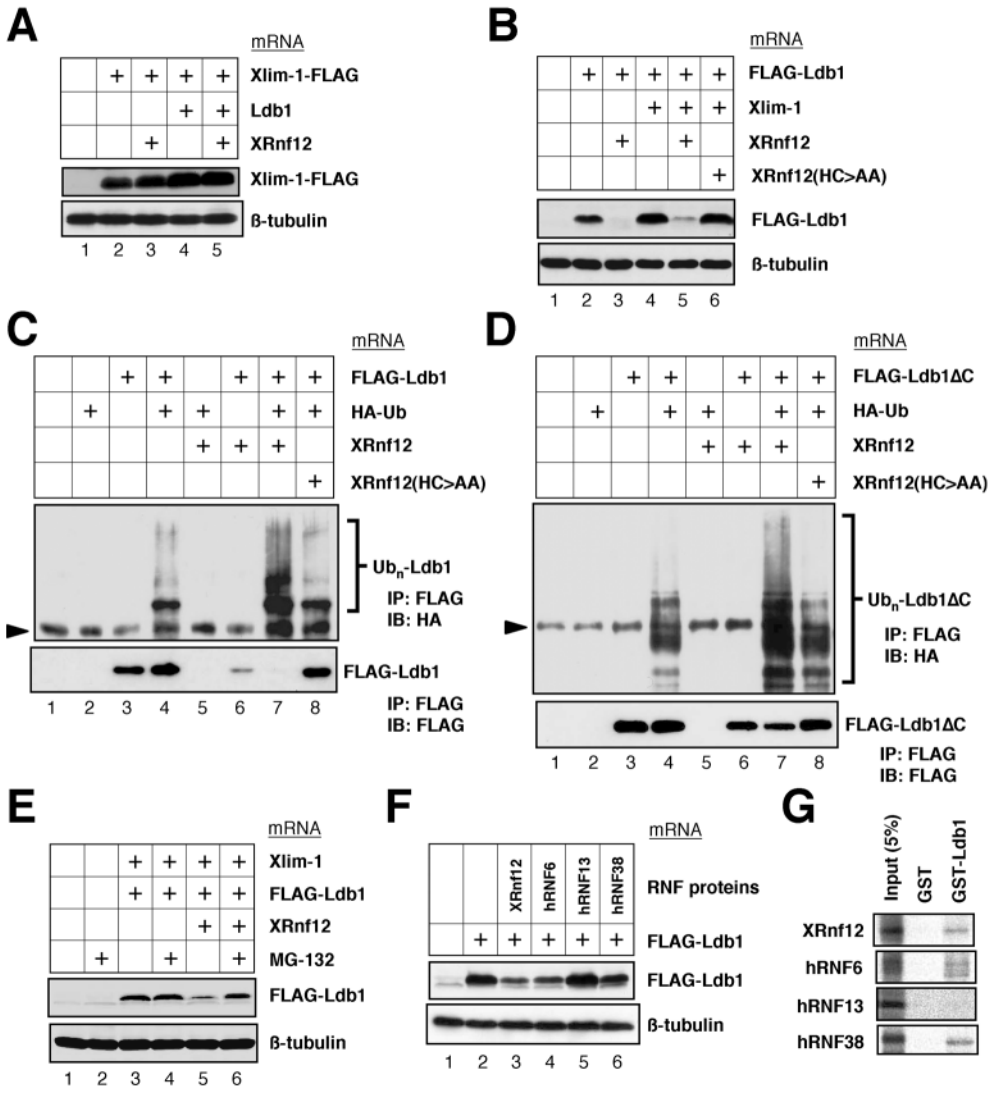

Fig. 4. XRnf12 causes ubiquitination and proteasome-dependent degradation of Ldb1 in a RING-dependent manner. (A) XRnf12 does not affect the steady-state level of Xlim-1-FLAG, either in the presence or absence of Ldb1. The indicated mRNAs were injected into the ventral region and the expression levels of the FLAG-tagged proteins were examined at the gastrula stage. Note that the levels of Xlim-1-FLAG are increased in the presence of Ldb1. β-tubulin, loading control. Amounts of mRNAs injected (ng/embryo): Xlim-1-FLAG, 0.25; Ldb1, 0.5; XRnf12, 0.25. (B) XRnf12 decreases the steady-state level of FLAG-Ldb1 both in the presence and absence of Xlim-1 in a RING-dependent manner. Note the increase in the expression level of FLAG-Ldb1 by Xlim-1 co-expression. Amounts of mRNAs (ng/embryo): FLAG-Ldb1, 0.5; Xlim-1, 0.25; XRnf12 constructs, 0.25. (C) XRnf12 enhances ubiquitination of Ldb1. Embryos were injected ventrally with the mRNAs indicated and the cell lysates were immunoprecipitated (IP) with anti-FLAG antibody followed by either anti-FLAG or anti-HA immunoblotting (IB) to detect non-ubiquitinated Ldb1 or ubiquitinated proteins, respectively. Co-expression of XRnf12 results in downregulation of non-ubiquitinated FLAG-Ldb1 expression levels (lower panel). While weak ubiquitination is observed in the absence of XRnf12 (lane 4), strong ladder-like ubiquitination signals appear in the presence of XRnf12 (lane 7). XRnf12(HC>AA) does not enhance ubiquitination (lane 8). Amounts of mRNAs (ng/embryo): FLAG-Ldb1, 2.0; HA-Ub, 1.0; XRnf12 constructs, 1.0. (D) The N-terminal region (aa 1-291) of Ldb1 is sufficient for ubiquitination by XRnf12. By using FLAG-Ldb1ΔC instead of FLAG-Ldb1, smaller-sized ubiquitinated protein bands are detected, confirming that the ubiquitinated proteins in C are indeed Ldb1 and not some other proteins associated with Ldb1. Co-expression of XRnf12 also results in downregulation of non-ubiquitinated FLAG-Ldb1ΔC. The amounts of mRNAs used are the same as in C. Arrowhead indicates the position of IgG. (E) XRnf12 causes proteasome-dependent degradation of Ldb1. After mRNA injection, cells were dispersed and cultured in the presence or absence of MG-132 until the gastrula stage. Decrease of FLAG-Ldb1 levels by XRnf12 (lane 5) is suppressed in the presence of MG-132 (lane 6). MG-132 does not affect the expression of FLAG-Ldb1 (lanes 3,4). Amounts of mRNAs (ng/embryo): FLAG-Ldb1, 0.5; Xlim-1, 0.25; XRnf12, 0.25. (F) The steady-state level of FLAG-Ldb1 is downregulated by hRNF6 and, to a lesser extent, by hRNF38, but not by hRNF13. The experimental design is the same as in A and B. β-tubulin, loading control. Amounts of mRNAs (ng/embryo): FLAG-Ldb1, 0.5; RING finger proteins, 0.5. (G) RING finger proteins that cause reduction in the steady-state level of Ldb1 interact with Ldb1. GST pull-down assay was performed with ^{35}S-labeled XRnf12, hRNF6, hRNF13 and hRNF38. Human RNF13 does not interact with GST-Ldb1, while other RING finger proteins do. GST serves as a negative control.

observe ubiquitination of Xlim-1 by XRnf12 (data not shown), consistent with the fact that XRnf12 does not alter the expression level of Xlim-1-FLAG (Fig. 4A). These data suggest that XRnf12 functions as a ubiquitin ligase specific to Ldb1, confirming a recent report on its mouse counterpart (Ostendorff et al., 2002). The weak intrinsic ubiquitin ligase activity toward Ldb1 (Fig. 4C, upper panel, lane 4) may be due to endogenous XRnf12.

We further examined whether XRnf12 mediates Ldb1 degradation by the proteasome. We co-expressed FLAG-Ldb1, Xlim-1, and XRnf12 ventrally, dispersed embryos into single cells, and cultured them in the presence of the proteasome inhibitor MG-132 until the gastrula stage. XRnf12-mediated reduction of FLAG-Ldb1 showed suppression in the presence of MG-132 (Fig. 4E, lane 6). MG-132 treatment alone had little or no effect on FLAG-Ldb1 expression (Fig. 4E, lanes 3,4). These results suggest that XRnf12 causes degradation of Ldb1 by the proteasome, also confirming the recent report on its mouse counterpart (Ostendorff et al., 2002).

To test the specificity of XRnf12, we analyzed three other related RING finger proteins, human RNF6, RNF38 and RNF13, for their ability to reduce Ldb1 expression levels. These three human proteins were chosen because they showed highest similarity to XRnf12 from database searching. Amino acid sequence identities of hRNF6, hRNF38 and hRNF13 to XRnf12 are 42%, 22% and 16% in entire proteins, and 80%, 51%, and 55% in the RING fingers, respectively. As shown in Fig. 4F, hRNF6 caused reduction in FLAG-Ldb1 expression levels, which seemed reasonable because of the relatively high sequence similarity between hRNF6 and XRnf12. That hRNF38 also caused reduction in FLAG-Ldb1 expression levels, albeit to a lesser extent, was somewhat unexpected, but the observed interaction between Ldb1 and hRNF38 in a GST pull-down assay provides a possible explanation for the activity of hRNF38 as well as hRNF6 (Fig. 4G). Human RNF13, which is the least similar to XRnf12 in the entire region of the three Rnf12-related proteins tested, did not interact with Ldb1 or affect its expression (Fig. 4F,G). These results suggest that not all Rnf12-related RING finger proteins can be involved in Ldb1 degradation, indicating that there is some degree of specificity in the activity of XRnf12.

Xlim-1 suppresses XRnf12-mediated degradation of Ldb1 through interaction with Ldb1

The fact that XRnf12 mediates ubiquitin-proteasome-dependent degradation of Ldb1 raises important questions. First, how is the activity of Xlim-1/Ldb1, which is apparently required in the organizer, assured in the presence of XRnf12? Second, what is the functional significance of Ldb1 degradation by XRnf12?

A clue to the first question came from our observation that co-expression of Xlim-1 reproducibly caused an increase in the expression level of FLAG-Ldb1 (Fig. 4B, compare lanes 2 and 4). As shown in Fig. 5A, we further confirmed that Xlim-1 dose-dependently increased the expression level of FLAG-Ldb1 (lanes 8-12), which may result from interfering with endogenous XRnf12. Moreover, we found that Xlim-1 suppressed XRnf12-mediated reduction of FLAG-Ldb1 levels in a dose-dependent manner (Fig. 5A, lanes 3-7). While the expression level of FLAG-Ldb1 became saturated in our range of Xlim-1 dosages in the absence of XRnf12 (Fig. 5A, lanes 11,12), it continued to increase at the same Xlim-1 dosages in the presence of XRnf12 (Fig. 5A, lanes 6,7). These results suggest that Xlim-1 suppresses the degradation of Ldb1 caused by exogenous XRnf12 and possibly endogenous XRnf12, implying mutual interactions between the three proteins.

To define the region in Xlim-1 required for this suppression, we expressed a series of Xlim-1 deletion constructs together with FLAG-Ldb1 and XRnf12, and examined the expression level of FLAG-Ldb1. Of all the constructs tested, only the LIM domain-containing ABL60 efficiently suppressed degradation of Ldb1 caused by XRnf12 (Fig. 5B, lane 5). Mouse LMO2 (Foroni et al., 1992) also suppressed degradation of Ldb1 caused by XRnf12 (Fig. 5C), although the interpretation of this result is complicated a little by the reported ubiquitin ligase activity of Rnf12 toward LMO2 (see Discussion). We conclude from our results that LIM domains are sufficient for the inhibition of XRnf12 activity.

We next defined the XRnf12-binding region in Xlim-1 by GST pull-down assay using a series of GST-Xlim-1 constructs and ^{35}S-labeled XRnf12. Contrary to the reported LIM domain-binding of mouse Rnf12 (Bach et al., 1999), the LIM domain-containing ABL60 showed virtually no interaction with XRnf12 (Fig. 5D). In contrast, the homeodomain-containing HD27 and ΔNA showed weak interactions with XRnf12 (Fig. 5D). Thus, the homeodomain-containing region (aa 178-265) of Xlim-1 is necessary and sufficient for the interaction with XRnf12 (Fig. 5E). Under our experimental conditions, GST-Xlim-1 showed a weaker affinity for XRnf12 than GST-Ldb1 (Fig. 5D). We also noticed that XRnf12 interacts with itself through the C-terminal region (aa 282-616) (Fig. 5D, GST-XRnf12ΔN), suggesting that XRnf12 may form a homodimeric complex.

Taken together, the LIM domain-containing region of Xlim-1, which is required for the interaction with Ldb1 (Agulnick et al., 1996; Breen et al., 1998) but not XRnf12, is sufficient for the suppression of XRnf12-mediated Ldb1 degradation. This suggests that binding of Xlim-1 to Ldb1 is a requisite for the suppression. We further tested this possibility by using FLAG-Ldb1ΔC, which does not contain the LIM interaction domain (Jurata and Gill, 1997; Breen et al., 1998). FLAG-Ldb1ΔC contains the region required for ubiquitination (Fig. 4D) and RING finger-dependent degradation by XRnf12 (Fig. 5F, lanes 2,3,6). In striking contrast to FLAG-Ldb1, XRnf12-mediated degradation of FLAG-Ldb1ΔC was not suppressed by Xlim-1 or other Xlim-1 constructs tested in Fig. 5B (Fig. 5F lanes 4,5 and data not shown), further supporting our hypothesis that binding of Xlim-1 to Ldb1 is required for the suppression. These results suggest that Ldb1 escapes degradation by XRnf12 upon association with Xlim-1, providing a plausible explanation of the way in which Xlim-1/Ldb1 could exert its effect in the presence of XRnf12 in the organizer.

No apparent dorsal-to-ventral (D/V) difference in the expression levels of the Ldb1 protein

Because Xlim-1 is enriched in the dorsal mesoderm, our results suggest that Ldb1 may be subject to selective degradation by XRnf12 in the ventrolateral mesoderm, thus contributing to further spatial restriction of Xlim-1 activity to the dorsalmost region. We addressed this question by using an anti-Ldb1 antibody, N-18, which recognizes a peptide sequence mapping at the conserved N terminus of vertebrate Ldb1. Specificity of

the antibody to the *Xenopus* Ldb1 protein was assessed by immunoblotting of *Xenopus* embryo extracts, which expressed a single band of a predicted size of approximately 46 kDa. Furthermore, exogenous Ldb1 expression by mRNA injection enhanced this 46 kDa band, whereas addition of blocking peptides at 1 μg/ml eliminated immunoreactivity, reflecting

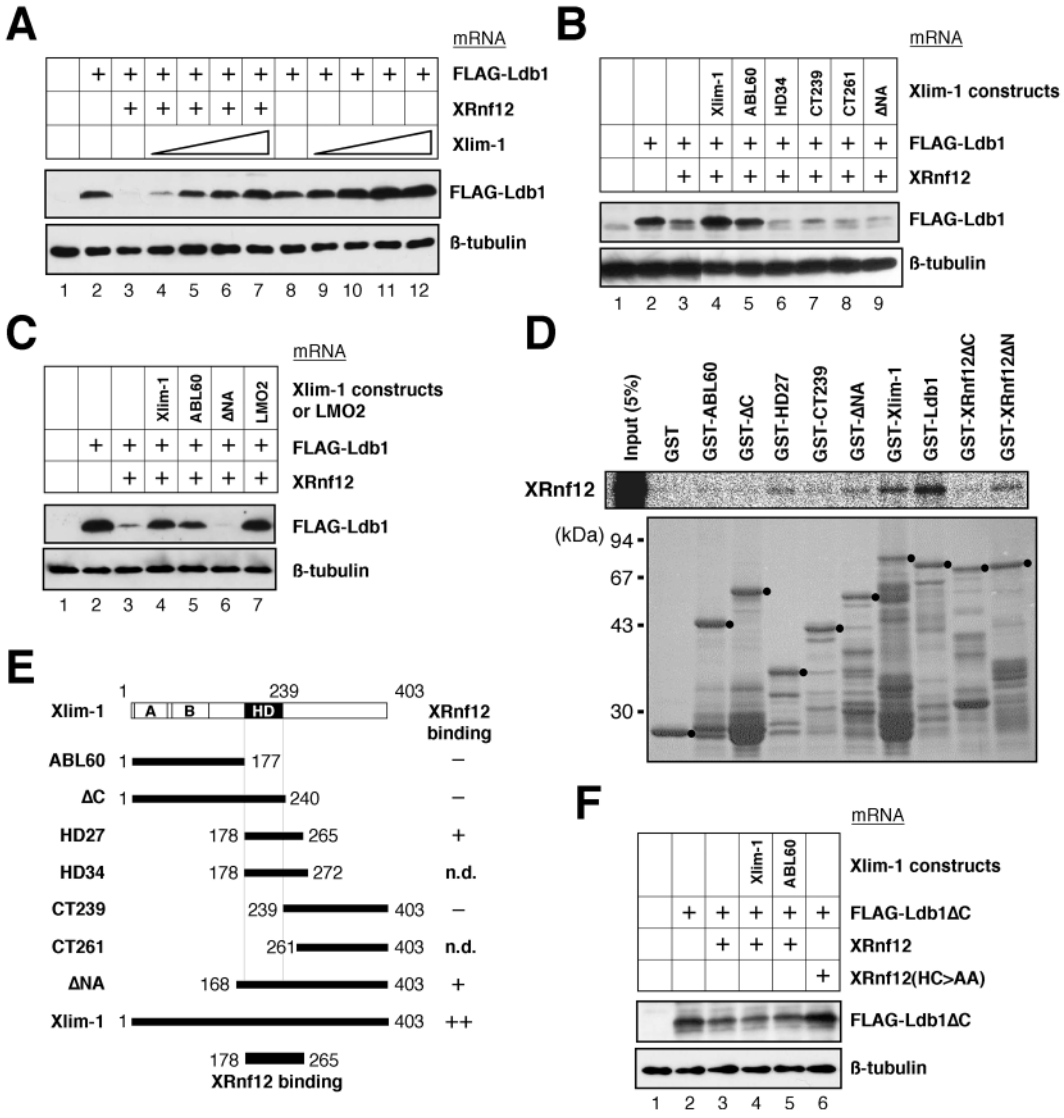

Fig. 5. A high level of Xlim-1 suppresses XRnf12-mediated degradation of Ldb1 through interaction with Ldb1. (A) Effects of Xlim-1 on XRnf12-mediated degradation of Ldb1. The experimental design is the same as in Fig. 4A,B. Xlim-1 increases the expression level of FLAG-Ldb1 dose-dependently in the presence (lanes 3-7) or absence (lanes 8-12) of XRnf12. Comparison between lanes 6 and 7, and lanes 11 and 12 suggests that Xlim-1 suppresses Ldb1 degradation by XRnf12. See text for details. Amounts of mRNAs (ng/embryo): FLAG-Ldb1, 0.5; XRnf12, 0.25; Xlim-1, 0.25 (lanes 4,9), 0.5 (lanes 5,10), 1.0 (lanes 6,11), 2.0 (lanes 7,12). (B) The LIM domain-containing fragment (ABL60) of Xlim-1 is sufficient for the suppression of XRnf12-mediated degradation of Ldb1. A series of Xlim-1 constructs depicted in E were tested at the highest dose used in A (lanes 7,12) for their ability to block Ldb1 degradation by XRnf12. ABL60, which contains the LIM domains, efficiently blocks Ldb1 degradation whereas other constructs does not. Amounts of mRNAs (ng/embryo): FLAG-Ldb1, 0.5; XRnf12, 0.25; Xlim-1 constructs, 2.0. (C) LIM-only protein LMO2 also efficiently blocks Ldb1 degradation in a different set of experiments designed as in B. (D) Interactions between ^{35}S-labeled XRnf12 and a series of GST-Xlim-1 constructs depicted in E were analyzed by GST pull-down assay. XRnf12 shows weak interactions with GST-HD27 and GST-ΔNA, while other GST-Xlim-1 constructs shows little or no interaction with XRnf12. GST-Ldb1 shows stronger interaction with XRnf12 than GST-Xlim-1 does. XRnf12 also shows weak self-interaction with GST-XRnf12ΔN (aa 282-616). GST alone serves as a negative control. Coomassie brilliant blue staining (lower panel) shows comparable amounts of GST fusion proteins (indicated by dots) used in the assay. (E) Representation of the GST-Xlim-1 constructs used for mapping experiments and the summary of the results shown in D. The homeodomain-containing region (aa 178-265) of Xlim-1 is necessary and sufficient for the interaction with XRnf12. A, B, LIM domains A and B; HD, homeodomain; n.d., not done; numbers, amino acid positions. (F) The LIM interaction domain of Ldb1 is required for the suppression of XRnf12-mediated Ldb1 degradation by Xlim-1 as revealed by the use of FLAG-Ldb1ΔC. XRnf12 causes degradation of Ldb1ΔC in a RING-dependent manner, which is not suppressed by Xlim-1 or ABL60. To avoid an overlap with a non-specific band, we used anti-Ldb1/CLIM2 (N-18) antibody in F to detect FLAG-Ldb1ΔC instead of anti-FLAG antibody used in the rest of the experiments in Fig. 5. Amounts of mRNAs injected (ng/embryo): FLAG-Ldb1ΔC, 0.5; XRnf12 constructs, 0.5; Xlim-1 constructs, 2.0.

specificity (not shown). We also confirmed that endogenous Ldb1 expression in animal caps is downregulated by overexpression of XRnf12 in a RING-dependent fashion (Fig. 6A), consistent with the results using exogenous Ldb1 constructs (Figs 4, 5).

Explants from the ventral marginal zone (VMZ) or dorsal marginal zone (DMZ) were dissected from gastrula embryos, and protein extracts were subjected to anti-Ldb1 immunoblotting. We noticed little dorsal-to-ventral (DV) difference in Ldb1 expression levels throughout early to mid gastrula stages 10, 10.5 and 11 (Fig. 6B and data not shown). We further examined DV difference by whole-mount immunostaining of bisected mid gastrula stage embryos (stage 10.5). Because the N-18 antibody did not react with Ldb1 on hemisections, we tested anti-mouse Ldb1/NLI antibodies (Jurata et al., 1996), and found they cross reacted with *Xenopus* Ldb1. As shown in Fig. 6C, signals were again detected uniformly in the mesoderm and ectoderm, and weakly in the endoderm, and showed subcellular localization to the nuclei, as predicted (Agulnick et al., 1996). Taken together, these results suggest that Ldb1 is not subject to selective degradation by XRnf12 in the ventrolateral mesoderm, possibly because of the presence of a Ldb1-binding protein in the ventrolateral mesoderm. Such a ventrally expressed Ldb1-interacting factor could be the LIM-only protein, XLMO4 (J. L.Gomez-Skarmeta, personal communication; see Discussion).

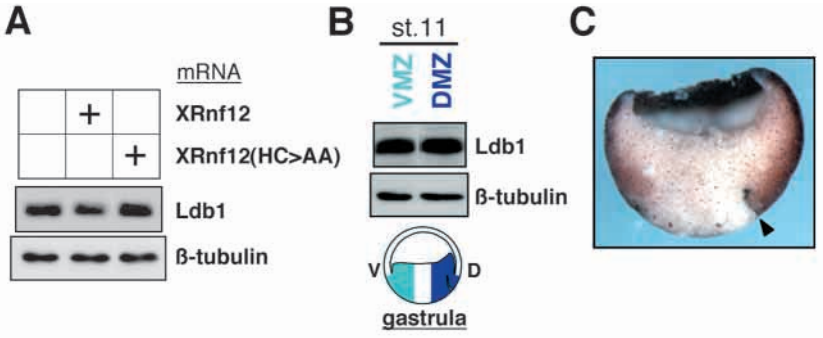

Fig. 6. Analysis of endogenous Ldb1 protein levels. (A) XRnf12 downregulates endogenous Ldb1 expression level in a RING-dependent manner. Animal caps were dissected at the blastula stage (stage 8-9) from embryos injected with the mRNAs (2 ng/embryo) indicated, and collected at the gastrula stage (stage 11). Endogenous Ldb1 expression levels were analyzed by western blotting using anti-Ldb1/CLIM2 (N-18) antibody. (B) Ldb1 does not exhibit dorsal-to-ventral (DV) difference in protein expression levels as revealed by western blot analysis. DMZ and VMZ explants dissected at the gastrula stage (stage 11) were compared for Ldb1 expression using anti-Ldb1/CLIM2 (N-18) antibody. (C) Ldb1 is uniformly expressed in the bisected mid gastrula embryo as revealed by immunostaining using anti-Ldb1/NLI antibody. Animal side is to the top, dorsal to the right. Arrowhead indicates blastopore.

Excess Ldb1 suppresses the expression of Xlim-1 target genes, which is rescued by co-expression of XRnf12

We next hypothesized that the functional significance of Ldb1 degradation by XRnf12 may be to eliminate excess Ldb1 molecules. We first examined the effect of Ldb1 overexpression on the axis-inducing activity of Xlim-1 (Fig. 7). As previously reported (Agulnick et al., 1996; Hiratani et al., 2001), co-expression of Xlim-1 (0.25 ng mRNA/embryo) and Ldb1 (0.5 ng mRNA/embryo) initiated secondary axis formation. Notably, excess amounts of Ldb1 (1.0 to 4.0 ng/embryo) inhibited this activity dose-dependently, whereas increasing the dose of Xlim-1 effectively suppressed the inhibitory action of excess amounts of Ldb1 (4.0 ng mRNA/embryo) (Fig. 7). These results suggest that the stoichiometry of Xlim-1 and Ldb1 is important for the exertion of their function, and that excess Ldb1 molecules are deleterious to Xlim-1. It is also possible that excess Ldb1 interferes with LIM domain-dependent association of Xlim-1 with other proteins, if any.

To further assess the likelihood of this hypothesis, we analyzed the effect of Ldb1 overexpression on the expression of candidate Xlim-1 targets, *gsc*, *chd*, *Xotx2*, *cerberus* (*cer*), and *Paraxial protocadherin* (*XPAPC*) (Taira et al., 1994b; Taira et al., 1997; Mochizuki et al., 2000; Hukriede et al., 2003; Yamamoto et al., 2003), as well as other organizer genes, *XFKH1*, *Xnot* and *dickkopf1* (*dkk1*) (Dirksen and Jamrich, 1992; von Dassow et al., 1993; Glinka et al., 1998). Pan-

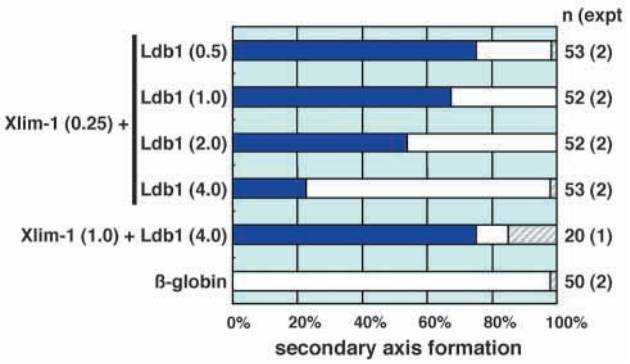

Fig. 7. Disturbing Xlim-1/Ldb1 stoichiometry affects their axis inducing activity. Ldb1 dose-dependently suppresses axis duplication by Xlim-1, which is rescued by co-expression of a higher dose (1 ng) of Xlim-1. Embryos injected with the mRNAs indicated were scored for axis development at the tailbud stage as in Fig. 3A. β-globin (2.0 ng/embryo) serves as a negative control. n, total number of injected embryos; expt, number of independent experiments. Amounts of mRNAs injected are indicated in parentheses (ng/embryo).

mesodermal and pan-mesendodermal markers, *Xbra* and *Mix.1*, respectively (Rosa, 1989; Smith et al., 1991), were also examined. As shown in Fig. 8, the patterns of alterations in gene expression could be categorized roughly into three groups. Group 1 is composed of genes that are downregulated by overexpression of either Ldb1 or XRnf12 alone (Fig. 8A-E), but restored by their co-expression in a RING-dependent manner (*gsc*, *chd*, *Xotx2*, *XPAPC* and *cer*). We found that genes reported as targets or candidate targets of Xlim-1 are all categorized into group 1. We have recently shown that *cer* expression is regulated by a complex of Xlim-1, Siamois and Mix.1 in a LIM domain-dependent fashion that does not involve Ldb1 (Yamamoto et al., 2003). Therefore, the effect of

Ldb1 on *cer* expression could be explained by disruption of the LIM domain-dependent transcription factor complex, as has been exemplified in the case of complex formation by the LIM-HD protein Lmx1 and the bHLH protein E47, which is disrupted by Ldb1 (Jurata and Gill, 1997). In contrast, there is no simple explanation for the effect of XRnf12 overexpression on *cer* expression, but it may result from some uncharacterized roles of the pleiotropic factor Ldb1 (Mukhopadhyay et al., 2003) in *cer* regulation. Nevertheless, these results are generally consistent with the idea that XRnf12 indirectly contributes to organizer gene expression through elimination of excess Ldb1 molecules, which are supposed to disturb Xlim-1/Ldb1 stoichiometry.

We also observed two other types of gene response to overexpression of Ldb1 and XRnf12. Group 2 contains genes that are downregulated by XRnf12 overexpression but not by Ldb1, and the effect of XRnf12 was suppressed by co-expression of Ldb1 (*XFKH1* and *Xnot*, Fig. 8F,G,). Group 3 is composed of genes that are downregulated (*dkk1* and *Mix.1*, Fig. 8H,I) or slightly affected (*Xbra*, Fig. 8J) by Ldb1 overexpression, but not by XRnf12. The effect on *Xbra* was relatively weak, compared to other genes, implying only a partial contribution of Ldb1, if any. Although there are no convincing explanations for the phenotypes of groups 2 and 3 at present (see Discussion), co-expression of Ldb1 and XRnf12 always restores the expression of the genes in groups 2 and 3 as well as those in group 1. This emphasizes the specificity of XRnf12 toward Ldb1 as well as the importance of maintaining the expression of Ldb1 to a proper level.

Ldb1 overexpression affects the maintenance phase of organizer gene expression

Our previous study suggests a role for Xlim-1 in the maintenance phase of organizer gene expression rather than initiation (Mochizuki et al., 2000). Therefore, we analyzed the effect of

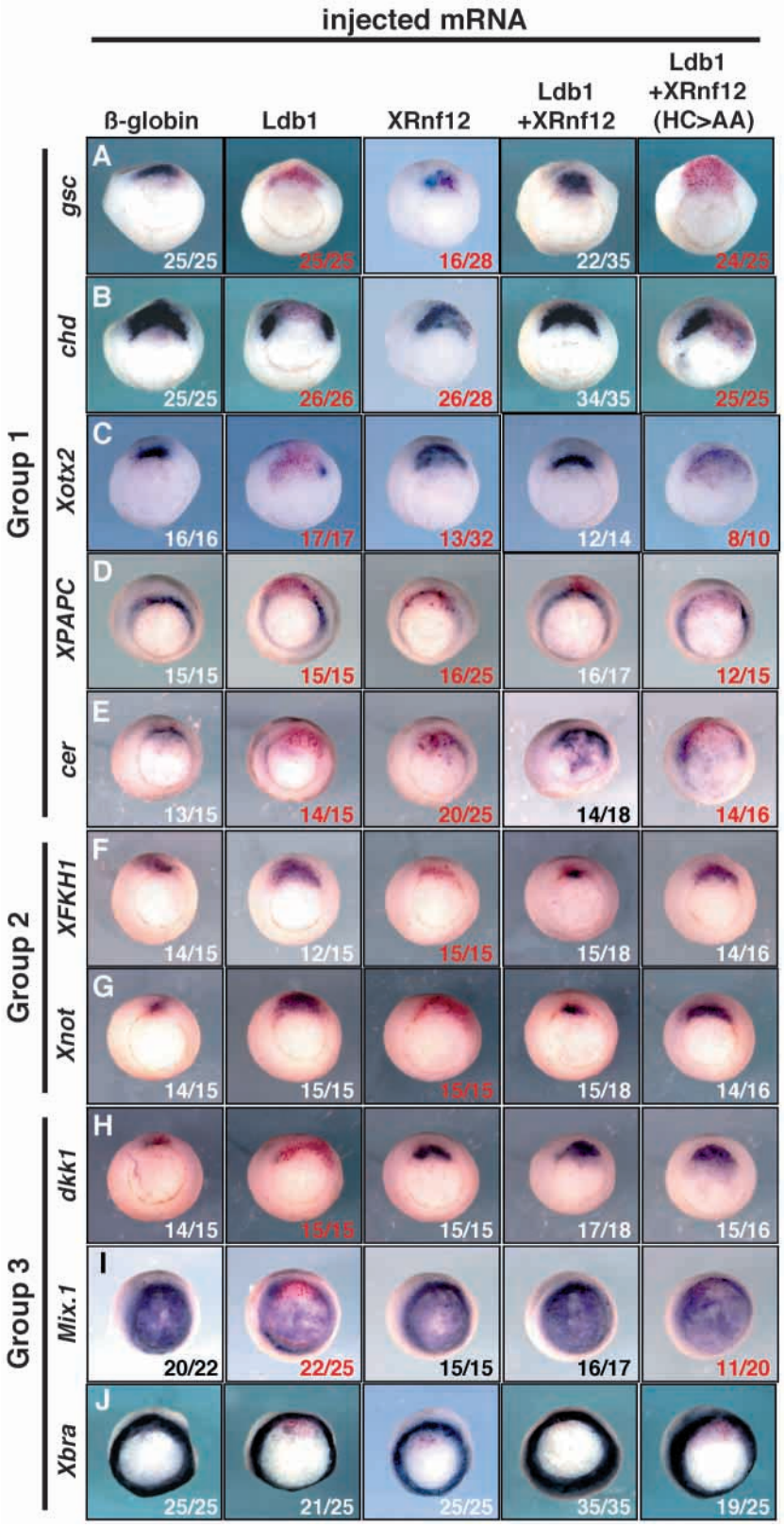

Fig. 8. Effects of Ldb1 or XRnf12 overexpression on organizer gene expression. Embryos injected dorsally with the mRNAs indicated were scored for expression of various marker genes in the organizer as assayed by whole-mount in situ hybridization. Genes categorized in group 1 (A-E, *gsc*, *chd*, *Xotx2*, *XPAPC* and *cer*) are downregulated by overexpression of either Ldb1 or XRnf12, whereas genes categorized in group 2 (F,G, *XFKH1* and *Xnot*) are downregulated only by XRnf12, and those in group 3 (H,I, *dkk1* and *Mix.1*) are downregulated only by Ldb1. *Xbra* (J) is only slightly affected by Ldb1 overexpression. Numbers indicate the frequency of the phenotype observed: numbers in red indicates downregulation, whereas numbers in black or white indicates normal expression. Note that downregulation of gene expression by either Ldb1 or XRnf12 overexpression was restored upon co-expression of both, and that the rescuing effect of XRnf12 co-expression was RING-dependent (except for *dkk1*, see Discussion). nβ-gal mRNA was coinjected as a lineage tracer, stained in red. Amounts of mRNAs (ng/embryo): nβ-gal, 0.06; β-globin, 4.0; Ldb1, 4.0; XRnf12, 2.0 or 4.0; XRnf12 constructs coinjected with Ldb1, 1.0 or 2.0.

Ldb1 overexpression on *gsc* expression during late blastula to mid gastrula stages (stages 9.5, 10, 10.5, and 11) to see if Ldb1 overexpression primarily affected the maintenance phase. Embryos were injected dorsally with *Ldb1* mRNA and RNA was then isolated from these embryos at stages 9.5, 10, 10.5 and 11 and subjected to RT-PCR analysis. As shown in Fig. 9, downregulation of *gsc* by Ldb1 overexpression was prominent at stages 10.5 and 11, whereas the effect was not as prominent at stages 9.5 and 10. Consistent with the results in Fig. 8, the reduction of *gsc* expression at stages 10.5 and 11 was suppressed by co-expression of XRnf12. These data support the idea that Ldb1 overexpression primarily affected the maintenance phase of *gsc* expression elicited by Xlim-1 rather than initiation.

DISCUSSION

Role of XRnf12 in gene regulation by Xlim-1 and Ldb1 in the organizer

In this study, we have analyzed the role of XRnf12 in the regulation of the activity of Xlim-1/Ldb1 in the Spemann organizer. Our initial overexpression study suggested a role for XRnf12 in negative regulation of Xlim-1/Ldb1 through Ldb1 degradation (Fig. 3), in agreement with a recent report on its mouse counterpart (Ostendorff et al., 2002). However, we have further shown that: (1) overexpression of Ldb1 suppresses axis duplication elicited by Xlim-1/Ldb1 (Fig. 7) as well as the expression of Xlim-1 target genes in the organizer (Fig. 8); (2) co-expression of XRnf12 rescues the effect of Ldb1 overexpression on putative Xlim-1 targets in a RING-dependent manner (Fig. 8); (3) ubiquitination-mediated degradation of Ldb1 by XRnf12 is inhibited by Xlim-1 through association of its LIM domains with the LIM interaction domain of Ldb1 (Fig. 5). Therefore, we propose a role for XRnf12 in selective degradation of excess Ldb1 molecules unbound to Xlim-1, which contributes to the establishment of proper Xlim-1/Ldb1 stoichiometry for the formation of functional Xlim-1/Ldb1 complex (Fig. 10).

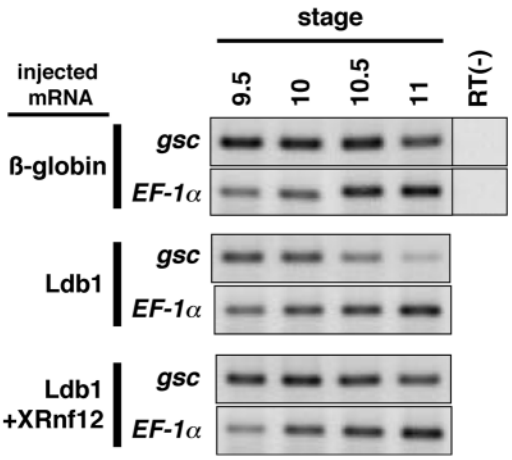

Fig. 9. Ldb1 overexpression affects the maintenance phase of *gsc* expression. Embryos injected dorsally with the mRNAs (4.0 ng/embryo) indicated were collected at stages 9.5, 10, 10.5 and 11 (late blastula to mid gastrula) and the expression of *gsc* was analyzed by RT-PCR. Downregulation of *gsc* by Ldb1 overexpression was not prominent at early-gastrula stages (st 9.5, 10) but became prominent after mid gastrula (stage 10.5, 11). Co-expression of XRnf12 restored *gsc* expression. *EF-1α* serves as a loading control.

We assume that Xlim-1/Ldb1 tetramer is the functional complex in the dorsal mesoderm (Figs 7, 10) (Hiratani et al., 2001), as has been suggested in the case of *Drosophila* LIM-HD Apterous and Chip/dLDB (Milan and Cohen, 1999; van Meyel et al., 1999; Rincon-Limas et al., 2000). This is also supported by the observation that overexpression of Ldb1ΔC, which is expected to disturb Xlim-1/Ldb1 tetramer formation, in the dorsal marginal zone (2 ng/embryo) leads to downregulation of putative Xlim-1 targets, *gsc* and *chd* (data not shown). The importance of LIM-HD/Ldb stoichiometry has also been dealt with in the case of Apterous and Chip/dLDB (Fernandez-Funez et al., 1998; Milan and Cohen, 1999; van Meyel et al., 1999).

We have shown that overexpression of Ldb1 or XRnf12 affects expression of candidate Xlim-1 target genes, *gsc*, *chd*, *Xotx2*, *XPAPC* and *cer* (Fig. 8, group 1). However, we have also noticed that overexpression of either XRnf12 (group 2) or Ldb1 (group 3) affects the expression of genes that have not been shown to be regulated by Xlim-1 and Ldb1 (Fig. 8, groups 2 and 3). Possible explanations for this observation with the group 2 and 3 genes are as follows: (1) The group 2 genes may be regulated by a Ldb1-containing complex which is disrupted by XRnf12 but not by excess amounts of Ldb1, and (2) *Mix.1* and *dkk1* in group 3 may be regulated by a Ldb1-independent complex, but this complex is disrupted by excess Ldb1 through Ldb1-interacting components in the complex, similar to the case of the *cer* gene. Curiously, inhibition of *dkk1* expression by Ldb1 was also rescued by XRnf12(HC>AA) (Fig. 8H). Binding of XRnf12(HC>AA) to Ldb1 may suffice to suppress the effect of excess Ldb1 in this case. Although these possibilities remain to be elucidated, it should be emphasized that the expression of candidate Xlim-1 target genes, but not other genes examined, are affected by both Ldb1 and XRnf12. In addition, because the effect of excess Ldb1 on the expression of group 3 genes was relatively small compared to that on group 1 genes, it seems that Ldb1 overexpression primarily affects dorsal mesodermal gene expression by Xlim-1. Most importantly, all the genes examined show normal expression upon co-expression of Ldb1 and XRnf12, supporting the requirement of proper expression levels of Ldb1, which may be assured in the presence of XRnf12.

Roles of XRnf12 in other developmental contexts

XRnf12 and *Ldb1* are expressed in a similar fashion throughout early developmental stages (Fig. 2). This is reminiscent of the term ‘synexpression group’ (Niehrs and Pollet, 1999), supporting the close functional interactions between Ldb1 and XRnf12. Because Ldb1 seems to escape degradation by binding to Xlim-1, we first assumed a dorsal-to-ventral gradient of Ldb1 protein expression, according to the distribution of Xlim-1 protein (Karavanov et al., 1996). This seems not to be the case, as we did not observe dorsal-to-ventral difference in Ldb1 expression levels (Fig. 6B,C). This result raises the possibility that Ldb1-interacting proteins other than Xlim-1, which could bind and protect Ldb1 from degradation, are present in the lateral and ventral regions as well as in the animal pole region (Fig. 10). This possibility could be explained by the presence of XLMO4 in the

ventrolateral mesoderm of the *Xenopus* embryo (J. L. Gomez-Skarmeta, personal communication) and Xlim-5 in the animal pole region (Toyama et al., 1995). In the ventrolateral mesoderm, Ldb1 may participate in a transcriptional regulatory complex that contains XLMO4 and perhaps GATA proteins, by analogy with the case of Ldb1, LMO2, and GATA-1 in blood development (Osada et al., 1995; Wadman et al., 1997). Because mouse LMO2, which is related to XLMO4, can block degradation of Ldb1 by XRnf12 (Fig. 5C), it is possible that LMO proteins [LMO1-4 (reviewed by Bach, 2000)] also utilize XRnf12 to acquire proper LMO/Ldb1 stoichiometry.

During the course of neuronal differentiation in the neural tube, several LIM-HD proteins are expressed to generate a so-called LIM code that is thought to define neuronal identity (Lumsden, 1995; Tanabe and Jessell, 1996). LIM-HD proteins are also involved in brain development (Sheng et al., 1996; Porter et al., 1997; Zhao et al., 1999). Interestingly, it has recently been shown that LIM-HD/Ldb1 stoichiometry appears to be important for the specification of motor neuron and interneuron identity by Lhx3/Islet-1/Ldb1 and Lhx3/Ldb1, respectively (Thaler et al., 2002). Because XRnf12 and Ldb1 are co-expressed in the brain and the spinal cord (Fig. 2), XRnf12 may contribute to LIM-HD/Ldb1 stoichiometry in these regions as well.

Regulation of protein stability by mutual interactions

In the *Drosophila* wing disc, complex formation between Apterous and Chip/dLDB attenuates proteasome-dependent degradation of Apterous and stabilizes Apterous protein (Weihe et al., 2001). Interestingly, we also noticed an increase in the expression level of Xlim-1 by Ldb1 co-expression (Fig. 4A, compare lanes 2,3 with lanes 4,5), suggesting that a similar mechanism for stabilization of Xlim-1 protein exists in vertebrates. Therefore, Xlim-1 may be more susceptible to proteasome-mediated degradation by some unknown factor(s) when not bound to Ldb1. This may contribute to the establishment of proper Xlim-1/Ldb1 stoichiometry dorsally, or may contribute to complete elimination of Xlim-1 protein ventrally (Fig. 10). Notably, similar protein stabilization by heterodimerization has been reported for the yeast transcription factors MATα2/MATa1 (Johnson et al., 1998) and for the *Drosophila* homeodomain proteins Homothorax and Extradenticle (Abu-Shaar and Mann, 1998).

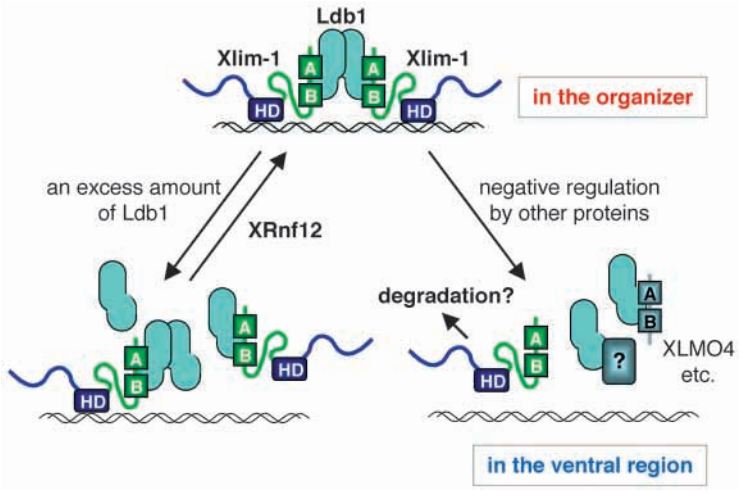

Fig. 10. A model for the role of XRnf12 in the establishment of proper Xlim-1/Ldb1 stoichiometry in the Spemann organizer. In the organizer, tetramer formation of Xlim-1/Ldb1 is required for their activity. XRnf12 selectively degrades excess Ldb1 unbound to Xlim-1, which interferes with organizer gene expression presumably by disturbing Xlim-1/Ldb1 tetramer formation. Excess Ldb1 may also possibly interfere with LIM domain-dependent association of Xlim-1 with other proteins. In this way, proper stoichiometry and maximal activity of Xlim-1/Ldb1 is assured in the presence of XRnf12 in the organizer. In the ventrolateral mesoderm, Ldb1 may escape degradation by XRnf12 through interaction with Ldb1-interacting proteins, one of which may be XLMO4 (J. L. Gomez-Skarmeta, personal communication). The putative Ldb1/LMO complex may contribute to complete suppression of Xlim-1/Ldb1 activity in the ventrolateral region, and may participate in a distinct transcriptional regulatory complex. Xlim-1 unbound to Ldb1 may be subject to proteasome-dependent degradation by an unidentified ubiquitin ligase, similar to the case of *Drosophila* Apterous (Weihe et al., 2001).

Cofactor exchange or maintenance of stoichiometry?

Ostendorff et al. proposed a model showing that Rnf12 mediates degradation of Ldb1/CLIM2 in complex with Lhx3 on the promoter region, thereby replacing Ldb1/CLIM2 with other cofactors (Ostendorff et al., 2002). However, this does not accord with our results that showed suppression of XRnf12-mediated degradation of Ldb1 by excess amounts of Xlim-1. It was also reported that Rnf12 regulates the activity of Lhx3 by recruiting the histone deacetylase complex (Bach et al., 1999), and that this regulation is independent of its RING finger (Ostendorff et al., 2002). In contrast to Lhx3, the inhibitory effect of XRnf12 overexpression on the activity of Xlim-1 solely relied on its RING finger, suggesting that ubiquitin ligase activity toward Ldb1 is the primary cause of the inhibition. Thus, there seems to be some difference in the way in which Rnf12 regulates different LIM-HD transcription factors. Alternatively, the difference may be the result of the different experimental systems: *Xenopus* embryos and cell cultures. We also did not observe interaction between XRnf12 and the LIM domains of Xlim-1, contrary to the reported binding of mouse Rnf12 to LIM domains of LIM-HD proteins, Lhx2, Lhx3 and Isl-1 (Bach et al., 1999). This may imply a difference in the binding affinity between Rnf12 and different LIM-HD proteins. Alternatively, XRnf12 might actually interact with the LIM domains of Xlim-1, although this could not be observed under our experimental conditions. Thus, the molecular basis underlying the difference in Rnf12-mediated regulation of Lhx3 and Xlim-1 remains to be elucidated. The functional significance of the reported ubiquitination and degradation of LMO proteins by Rnf12/RLIM (Ostendorff et al., 2002), and the mechanisms by which Rnf12/RLIM distinguishes LMO proteins from LIM-HD proteins, are also important questions to be answered.

Nevertheless, the results so far seem to be in good agreement about the close functional interactions between LIM-HD, Ldb1 and Rnf12 proteins. We believe that our results expand the knowledge of LIM-HD regulation and provide an attractive possibility that multimeric transcriptional regulatory complex such as LIM-HD/Ldb1 complexes are regulated in a similar way in which selective degradation of excess transcription

factors or adapter proteins occurs through the ubiquitin-proteasome pathway for the establishment of their proper stoichiometry.

We thank the following for their generous contribution of reagents: B. Blumberg (a *Xenopus* gastrula cDNA library), D. Turner, R. Rupp and J. Lee (pCS2+ and pCS2+nβgal), E. De Robertis (*gsc*, *XPAPC*, and *cer*), Y. Sasai (*chd*), M. Pannese and E. Boncinelli (*Xotx2*), M. Jamrich (*XFKH1*), D. Kimelman (*Xnot*), F. Rosa (*Mix.1*), J. Smith (*Xbra*), M. Watanabe and M. Whitman (pCS2+3HA), H. Osada (LMO2), C. Niehrs (*dkk1*) and G. Gill (anti-NLI antibodies). We are also grateful to J. L. Gomez-Skarmeta for sharing unpublished results of XLMO4 analysis, N. Sugimoto for pSP64T-Xlim-5, M. Watanabe and M. Whitman for the bisection and coimmunoprecipitation protocols, J. Shinga for a *Xenopus* neurula cDNA library, S. Taira for sectioning, and M. Itoh, A. Takahashi and M. Inamori for whole-mount in situ hybridization. This work was supported in part by a Grant-in-Aid for Scientific Research from the Ministry of Education, Culture, Sports, Science and Technology of Japan, and by the Toray Science Foundation, Japan. I.H. is a research fellow of the Japan Society for the Promotion of Science.

REFERENCES

Abu-Shaar, M. and Mann, R. S. (1998). Generation of multiple antagonistic domains along the proximodistal axis during *Drosophila* leg development. *Development* **125**, 3821-3830.

Agulnick, A. D., Taira, M., Breen, J. J., Tanaka, T., Dawid, I. B. and Westphal, H. (1996). Interactions of the LIM-domain-binding factor Ldb1 with LIM homeodomain proteins. *Nature* **384**, 270-272.

Bach, I. (2000). The LIM domain: regulation by association. *Mech. Dev.* **91**, 5-17.

Bach, I., Carriere, C., Ostendorff, H. P., Andersen, B. and Rosenfeld, M. G. (1997). A family of LIM domain-associated cofactors confer transcriptional synergism between LIM and Otx homeodomain proteins. *Genes Dev.* **11**, 1370-1380.

Bach, I., Rodriguez-Esteban, C., Carriere, C., Bhushan, A., Krones, A., Rose, D. W., Glass, C. K., Andersen, B., Izpisua Belmonte, J. C. and Rosenfeld, M. G. (1999). RLIM inhibits functional activity of LIM homeodomain transcription factors via recruitment of the histone deacetylase complex. *Nat. Genet.* **22**, 394-399.

Bouwmeester, T. (2001). The Spemann-Mangold organizer: the control of fate specification and morphogenetic rearrangements during gastrulation in *Xenopus*. *Int. J. Dev. Biol.* **45**, 251-258.

Bouwmeester, T., Kim, S., Sasai, Y., Lu, B. and de Robertis, E. M. (1996). Cerberus is a head-inducing secreted factor expressed in the anterior endoderm of Spemann's organizer. *Nature* **382**, 595-601.

Breen, J. J., Agulnick, A. D., Westphal, H. and Dawid, I. B. (1998). Interactions between LIM domains and the LIM domain-binding protein Ldb1. *J. Biol. Chem.* **273**, 4712-4717.

Cho, K. W., Blumberg, B., Steinbeisser, H. and de Robertis, E. M. (1991). Molecular nature of Spemann's organizer: the role of the *Xenopus* homeobox gene *goosecoid*. *Cell* **67**, 1111-1120.

Dawid, I. B., Breen, J. J. and Toyama, R. (1998). LIM domains: multiple roles as adapters and functional modifiers in protein interactions. *Trends Genet.* **14**, 156-162.

De Robertis, E. M., Larrain, J., Oelgeschlager, M. and Wessely, O. (2000). The establishment of Spemann's organizer and patterning of the vertebrate embryo. *Nat. Rev. Genet.* **1**, 171-181.

Dirksen, M. L. and Jamrich, M. (1992). A novel, activin-inducible, blastopore lip-specific gene of *Xenopus laevis* contains a fork head DNA-binding domain. *Genes Dev.* **6**, 599-608.

Dworkin-Rastl, E., Shrutkowski, A. and Dworkin, M. B. (1984). Multiple ubiquitin mRNAs during *Xenopus laevis* development contain tandem repeats of the 76 amino acid coding sequence. *Cell* **39**, 321-325.

Fernandez-Funez, P., Lu, C. H., Rincon-Limas, D. E., Garcia-Bellido, A. and Botas, J. (1998). The relative expression amounts of apterous and its co-factor dLdb/Chip are critical for dorso-ventral compartmentalization in the *Drosophila* wing. *EMBO J.* **17**, 6846-6853.

Foroni, L., Boehm, T., White, L., Forster, A., Sherrington, P., Liao, X. B., Brannan, C. I., Jenkins, N. A., Copeland, N. G. and Rabbitts, T. H. (1992). The rhombotin gene family encode related LIM-domain proteins whose differing expression suggests multiple roles in mouse development. *J. Mol. Biol.* **226**, 747-761.

Glickman, M. H. and Ciechanover, A. (2002). The ubiquitin-proteasome proteolytic pathway: destruction for the sake of construction. *Physiol. Rev.* **82**, 373-428.

Glinka, A., Wu, W., Delius, H., Monaghan, A. P., Blumenstock, C. and Niehrs, C. (1998). Dickkopf-1 is a member of a new family of secreted proteins and functions in head induction. *Nature* **391**, 357-362.

Harland, R. and Gerhart, J. (1997). Formation and function of Spemann's organizer. *Annu. Rev. Cell Dev. Biol.* **13**, 611-667.

Harland, R. M. (1991). In situ hybridization: an improved whole-mount method for *Xenopus* embryos. *Methods Cell Biol.* **36**, 685-695.

Hershko, A. and Ciechanover, A. (1998). The ubiquitin system. *Annu. Rev. Biochem.* **67**, 425-479.

Hikasa, H. and Taira, M. (2001). A *Xenopus* homolog of a human p53-activated gene, *PA26*, is specifically expressed in the notochord. *Mech. Dev.* **100**, 309-312.

Hiratani, I., Mochizuki, T., Tochimoto, N. and Taira, M. (2001). Functional domains of the LIM homeodomain protein Xlim-1 involved in negative regulation, transactivation, and axis formation in *Xenopus* embryos. *Dev. Biol.* **229**, 456-467.

Hukriede, N. A., Tsang, T. E., Habas, R., Khoo, P. L., Steiner, K., Weeks, D. L., Tam, P. P. and Dawid, I. B. (2003). Conserved requirement of Lim1 function for cell movements during gastrulation. *Dev. Cell* **4**, 83-94.

Jackson, P. K., Eldridge, A. G., Freed, E., Furstenthal, L., Hsu, J. Y., Kaiser, B. K. and Reimann, J. D. (2000). The lore of the RINGs: substrate recognition and catalysis by ubiquitin ligases. *Trends Cell Biol.* **10**, 429-439.

Joazeiro, C. A. and Weissman, A. M. (2000). RING finger proteins: mediators of ubiquitin ligase activity. *Cell* **102**, 549-552.

Johnson, P. R., Swanson, R., Rakhilina, L. and Hochstrasser, M. (1998). Degradation signal masking by heterodimerization of MATα2 and MATa1 blocks their mutual destruction by the ubiquitin-proteasome pathway. *Cell* **94**, 217-227.

Jurata, L. W. and Gill, G. N. (1997). Functional analysis of the nuclear LIM domain interactor NLI. *Mol. Cell Biol.* **17**, 5688-5698.

Jurata, L. W., Kenny, D. A. and Gill, G. N. (1996). Nuclear LIM interactor, a rhombotin and LIM homeodomain interacting protein, is expressed early in neuronal development. *Proc. Natl. Acad. Sci. USA* **93**, 11693-11698.

Jurata, L. W., Pfaff, S. L. and Gill, G. N. (1998). The nuclear LIM domain interactor NLI mediates homo- and heterodimerization of LIM domain transcription factors. *J. Biol. Chem.* **273**, 3152-3157.

Karavanov, A. A., Saint-Jeannet, J. P., Karavanova, I., Taira, M. and Dawid, I. B. (1996). The LIM homeodomain protein Lim-1 is widely expressed in neural, neural crest and mesoderm derivatives in vertebrate development. *Int. J. Dev. Biol.* **40**, 453-461.

Kim, S. H., Yamamoto, A., Bouwmeester, T., Agius, E. and de Robertis, E. M. (1998). The role of paraxial protocadherin in selective adhesion and cell movements of the mesoderm during *Xenopus* gastrulation. *Development* **125**, 4681-4690.

Kodjabachian, L., Karavanov, A. A., Hikasa, H., Hukriede, N. A., Aoki, T., Taira, M. and Dawid, I. B. (2001). A study of Xlim1 function in the Spemann-Mangold organizer. *Int. J. Dev. Biol.* **45**, 209-218.

Krieg, P. A. and Melton, D. A. (1984). Functional messenger RNAs are produced by SP6 in vitro transcription of cloned cDNAs. *Nucleic Acids Res.* **12**, 7057-7070.

Lee, M. A., Heasman, J. and Whitman, M. (2001). Timing of endogenous activin-like signals and regional specification of the *Xenopus* embryo. *Development* **128**, 2939-2952.

Lumsden, A. (1995). Neural development. A 'LIM code' for motor neurons? *Curr. Biol.* **5**, 491-495.

Milan, M. and Cohen, S. M. (1999). Regulation of LIM homeodomain activity in vivo: a tetramer of dLDB and apterous confers activity and capacity for regulation by dLMO. *Mol. Cell* **4**, 267-273.

Mochizuki, T., Karavanov, A. A., Curtiss, P. E., Ault, K. T., Sugimoto, N., Watabe, T., Shiokawa, K., Jamrich, M., Cho, K. W., Dawid, I. B. et al. (2000). Xlim-1 and LIM domain binding protein 1 cooperate with various transcription factors in the regulation of the *goosecoid* promoter. *Dev. Biol.* **224**, 470-485.

Mukhopadhyay, M., Teufel, A., Yamashita, T., Agulnick, A. D., Chen, L., Downs, K. M., Schindler, A., Grinberg, A., Huang, S. P., Dorward, D. et al. (2003). Functional ablation of the mouse *Ldb1* gene results in severe patterning defects during gastrulation. *Development* **130**, 495-505.

Nakano, H., Amemiya, S., Shiokawa, K. and Taira, M. (2000). RNA interference for the organizer-specific gene *Xlim-1* in *Xenopus* embryos. *Biochem. Biophys. Res. Commun.* **274**, 434-439.

Niehrs, C. and Pollet, N. (1999). Synexpression groups in eukaryotes. *Nature* **402**, 483-487.

Osada, H., Grutz, G., Axelson, H., Forster, A. and Rabbitts, T. H. (1995). Association of erythroid transcription factors: complexes involving the LIM protein RBTN2 and the zinc-finger protein GATA1. *Proc. Natl. Acad. Sci. USA* **92**, 9585-9589.

Osada, S.-I., Ohmori, S.-y. and Taira, M. (2003). XMAN1, an inner nuclear membrane protein, antagonizes BMP signaling by interacting with Smad1 in *Xenopus* embryos. *Development* **130**, 1783-1794.

Ostendorff, H. P., Peirano, R. I., Peters, M. A., Schluter, A., Bossenz, M., Scheffner, M. and Bach, I. (2002). Ubiquitination-dependent cofactor exchange on LIM homeodomain transcription factors. *Nature* **416**, 99-103.

Pannese, M., Polo, C., Andreazzoli, M., Vignali, R., Kablar, B., Barsacchi, G. and Boncinelli, E. (1995). The *Xenopus* homologue of Otx2 is a maternal homeobox gene that demarcates and specifies anterior body regions. *Development* **121**, 707-720.

Porter, F. D., Drago, J., Xu, Y., Cheema, S. S., Wassif, C., Huang, S. P., Lee, E., Grinberg, A., Massalas, J. S., Bodine, D. et al. (1997). *Lhx2*, a Lim homeobox gene, is required for eye, forebrain, and definitive erythrocyte development. *Development* **124**, 2935-2944.

Rincon-Limas, D. E., Lu, C. H., Canal, I. and Botas, J. (2000). The level of DLDB/CHIP controls the activity of the LIM homeodomain protein apterous: evidence for a functional tetramer complex in vivo. *EMBO J.* **19**, 2602-2614.

Rosa, F. M. (1989). *Mix.1*, a homeobox mRNA inducible by mesoderm inducers, is expressed mostly in the presumptive endodermal cells of *Xenopus* embryos. *Cell* **57**, 965-974.

Sasai, Y., Lu, B., Steinbeisser, H. and de Robertis, E. M. (1995). Regulation of neural induction by the Chd and Bmp-4 antagonistic patterning signals in *Xenopus*. *Nature* **376**, 333-336.

Saurin, A. J., Borden, K. L., Boddy, M. N. and Freemont, P. S. (1996). Does this have a familiar RING? *Trends Biochem. Sci.* **21**, 208-214.

Schlosser, G. and Northcutt, R. G. (2000). Development of neurogenic placodes in *Xenopus laevis*. *J. Comp. Neurol.* **418**, 121-146.

Shawlot, W. and Behringer, R. R. (1995). Requirement for *Lim1* in head-organizer function. *Nature* **374**, 425-430.

Sheng, H. Z., Zhadanov, A. B., Mosinger, B., Jr, Fujii, T., Bertuzzi, S., Grinberg, A., Lee, E. J., Huang, S. P., Mahon, K. A. and Westphal, H. (1996). Specification of pituitary cell lineages by the LIM homeobox gene *Lhx3*. *Science* **272**, 1004-1007.

Shibata, M., Itoh, M., Ohmori, S.-y., Shinga, J. and Taira, M. (2001). Systematic screening and expression analysis of the head organizer genes in *Xenopus* embryos. *Dev. Biol.* **239**, 241-256.

Shinga, J., Itoh, M., Shiokawa, K., Taira, S. and Taira, M. (2001). Early patterning of the prospective midbrain-hindbrain boundary by the HES-related gene *XHR1* in *Xenopus* embryos. *Mech. Dev.* **109**, 225-239.

Smith, J. C., Price, B. M., Green, J. B., Weigel, D. and Herrmann, B. G. (1991). Expression of a *Xenopus* homolog of Brachyury (T) is an immediate-early response to mesoderm induction. *Cell* **67**, 79-87.

Taira, M., Jamrich, M., Good, P. J. and Dawid, I. B. (1992). The LIM domain-containing homeo box gene *Xlim-1* is expressed specifically in the organizer region of *Xenopus* gastrula embryos. *Genes Dev.* **6**, 356-366.

Taira, M., Otani, H., Jamrich, M. and Dawid, I. B. (1994a). Expression of the LIM class homeobox gene *Xlim-1* in pronephros and CNS cell lineages of *Xenopus* embryos is affected by retinoic acid and exogastrulation. *Development* **120**, 1525-1536.

Taira, M., Otani, H., Saint-Jeannet, J. P. and Dawid, I. B. (1994b). Role of the LIM class homeodomain protein Xlim-1 in neural and muscle induction by the Spemann organizer in *Xenopus*. *Nature* **372**, 677-679.

Taira, M., Saint-Jeannet, J. P. and Dawid, I. B. (1997). Role of the *Xlim-1* and *Xbra* genes in anteroposterior patterning of neural tissue by the head and trunk organizer. *Proc. Natl. Acad. Sci. USA* **94**, 895-900.

Tanabe, Y. and Jessell, T. M. (1996). Diversity and pattern in the developing spinal cord. *Science* **274**, 1115-1123.

Thaler, J. P., Lee, S. K., Jurata, L. W., Gill, G. N. and Pfaff, S. L. (2002). LIM factor Lhx3 contributes to the specification of motor neuron and interneuron identity through cell-type-specific protein-protein interactions. *Cell* **110**, 237-249.

Toyama, R., Curtiss, P. E., Otani, H., Kumura, M., Dawid, I. B. and Taira, M. (1995). The LIM class homeobox gene *lim5*: Implied role in CNS patterning in *Xenopus* and zebrafish. *Dev. Biol.* **170**, 583-593.

van Meyel, D. J., O'Keefe, D. D., Jurata, L. W., Thor, S., Gill, G. N. and Thomas, J. B. (1999). Chip and Apterous physically interact to form a functional complex during *Drosophila* development. *Mol. Cell* **4**, 259-265.

von Dassow, G., Schmidt, J. E. and Kimelman, D. (1993). Induction of the *Xenopus* organizer: expression and regulation of *Xnot*, a novel FGF and activin-regulated homeo box gene. *Genes Dev.* **7**, 355-366.

Wadman, I. A., Osada, H., Grutz, G. G., Agulnick, A. D., Westphal, H., Forster, A. and Rabbitts, T. H. (1997). The LIM-only protein Lmo2 is a bridging molecule assembling an erythroid, DNA-binding complex which includes the TAL1, E47, GATA-1 and Ldb1/NLI proteins. *EMBO J.* **16**, 3145-3157.

Watanabe, M. and Whitman, M. (1999). FAST-1 is a key maternal effector of mesoderm inducers in the early *Xenopus* embryo. *Development* **126**, 5621-5634.

Weihe, U., Milan, M. and Cohen, S. M. (2001). Regulation of Apterous activity in *Drosophila* wing development. *Development* **128**, 4615-4622.

Yamamoto, S., Hikasa, H., Ono, H. and Taira, M. (2003). Molecular link in the sequential induction of the Spemann organizer: direct activation of the *cerberus* gene by Xlim-1, Xotx2, Mix.1, and Siamois, immediately downstream from Nodal and Wnt signaling. *Dev. Biol.* **257**, 190-204.

Zhao, Y., Sheng, H. Z., Amini, R., Grinberg, A., Lee, E., Huang, S., Taira, M. and Westphal, H. (1999). Control of hippocampal morphogenesis and neuronal differentiation by the LIM homeobox gene *Lhx5*. *Science* **284**, 1155-1158.